Europe-wide atmospheric radionuclide dispersion by unprecedented wildfires in the Chernobyl Exclusion Zone, April 2020

Olivier Masson, Oleksandr Romanenko, Olivier Saunier, Serhii Kirieiev, Valentyn Protsak, Gennady Laptev, Oleg Voitsekhovych, Vanessa Durand, Frederic Coppin, Georg Steinhauser, et al.

Europe-wide atmospheric radionuclide dispersion by unprecedented wildfires in the Chernobyl Exclusion Zone, April 2020

Olivier Masson[1 *], Oleksandr Romanenko[2], Olivier Saunier[1], Serhii Kirieiev[3], Valentin Protsak[4], Gennady Laptev[4], Oleg Voitsekhovych[4], Vanessa Durand[1], Frédéric Coppin[1], Georg Steinhauser[5], Anne de Vismes Ott[1], Philippe Renaud[1], Damien Didier[1], Béatrice Boulet[1], Maxime Morin[1], Miroslav Hýža[6], Johan Camps[7], Olga Belyaeva[8], Axel Dalheimer[9], Konstantinos Eleftheriadis[10], Catalina Gascó-Leonarte[11], Alexandra Ioannidou[12], Krzysztof Isajenko[13], Tero Karhunen[14], Johan Kastlander[15], Christian Katzlberger[16], Renata Kierepko[17], Gert-Jan Knetsch[18], Júlia Kövendiné Kónyi[19], Jerzy Wojciech Mietelski[17], Michael Mirsch[9], Bredo Møller[20], Jelena Krneta Nikolić[21], Pavel Peter Povinec[22], Rosella Rusconi[23], Vladimir Samsonov[24], Ivan Sýkora[22], Elena Simion[25], Philipp Steinmann[26], Stylianos Stoulos[12], José Antonio Suarez-Navarro[11], Herbert Wershofen[27], Daniel Zapata-García[27], Benjamin Zorko[28]

1 Institut de Radioprotection et de Sûreté Nucléaire (IRSN), Fontenay-Aux-Roses, 92260, France, olivier.masson@irsn.fr
2 Rivne Nuclear Power Plant (ENERGOATOM), Varash, Rivne Region, 34400, Ukraine
3 State Specialized Enterprise Ecocentre (SSE ECOCENTRE), Chornobyl, Kiev region, 07270, Ukraine
4 Ukrainian Hydrometeorological Institute (UHMI), Kyiv, 03028, Ukraine
5 Institute of Radioecology and Radiation Protection, Leibniz Universität Hannover, Hannover, 30419, Germany
6 National Radiation Protection Institute (SÚRO), Prague 4, 140 00, Czech Republic
7 StudieCentrum voor Kernenergie - Centre d'Etude de l'Energie Nucléaire (SCK-CEN), 2400, Mol, Belgium
8 Center for Ecological-Noosphere Studies (NAS RA), Department of Radioecology, 0025 Yerevan, Armenia
9 Deutscher Wetterdienst (DWD), 63067 Offenbach, Germany
10 Institute of Nuclear and Radiological Sciences & Technology, Energy & Safety, National Centre for Scientific Research "Demokritos", Athens, 15310, Greece
11 Centro de Investigaciones Energéticas, Medioambientales y Tecnológicas (CIEMAT), Unidad de Radioactividad Ambiental y Vigilancia Radiológica, Madrid, 28040, Spain
12 Aristotle University of Thessaloniki, Nuclear Physics and Elementary Particle Physics Division, Physics Department, Thessaloniki, 54124, Greece
13 Central Laboratory for Radiological Protection (CLRP), Warsaw, PL 03-194, Poland
14 Radiation and Nuclear Safety Authority (STUK), PL 14, Helsinki, 00881, Finland
15 Swedish Defence Research Agency (FOI), 164 90 Stockholm, Sweden
16 Austrian Agency for Health and Food Safety (AGES), Department of Radiation Protection and Technical Quality Assurance, Vienna, 1220, Austria
17 The Henryk Nievodniczanski Institute of Nuclear Physics (IFJ), Polish Academy of Sciences, Kraków, 31-342, Poland
18 National Institute of Public Health and the Environment (RIVM), PO Box 1, Bilthoven, NL-3720 BA, The Netherlands
19 National Public Health Center, Department of Radiobiology and Radiohygiene (NNK SSFO), Budapest, H-1221, Hungary
20 Norwegian Radiation and Nuclear Safety Authority (DSA), Emergency Preparedness and Response, Svanvik, NO-9925, Norway
21 Vinča Institute of Nuclear Sciences, Department of Radiation and Environmental Protection, Belgrade, 11351, Serbia
22 Department of Nuclear Physics and Biophysics, Comenius University, Bratislava, 842 48, Slovakia
23 Centro Regionale Radioprotezione, Agenzia Regionale per la Protezione dell'Ambiente della Lombardia (ARPA Lombardia), 20124 Milan, Italy
24 National Center for Hydrometeorology, Radioactive Contamination Control, and Environmental Monitoring (BELHYDROMET), Minsk, 220114, Belarus
25 National Environmental Protection Agency (NEPA), National Reference Laboratory, Bucharest, 060031, Romania
26 Federal Office of Public Health (FOPH - OFSP), Environmental Radioactivity Section, Liebefeld, CH-3097, Switzerland
27 Physikalisch-Technische Bundesanstalt (PTB), Braunschweig, 38116, Germany
28 Institut "Jozef Stefan" (IJS), SI-100 Ljubljana, Slovenia

Keywords : Wildfire, radionuclides, Chernobyl, firefighters, dose assessment

Abstract

From early April 2020, wildfires raged in the highly contaminated areas around the Chernobyl nuclear power plant (CNPP), Ukraine. For about four weeks, the fires spread around and into the Chernobyl exclusion zone (CEZ) and came within a few kilometres of both the CNPP and radioactive waste storage facilities. Wildfires occurred on several occasions throughout the month of April. They were extinguished, but weather conditions and the spread of fires by airborne embers and smoldering fires led to new fires starting at different locations of the CEZ. The forest fires were only completely under control at the beginning of May, thanks to the tireless and incessant work of the firefighters and a period of sustained precipitation. In total, 0.7-1.2 TBq ^{137}Cs were released into the atmosphere. Smoke plumes partly spread south and west and contributed to the detection of airborne ^{137}Cs over the Ukrainian territory and as far away as Western Europe. The increase in airborne ^{137}Cs ranged from several hundred $\mu Bq \cdot m^{-3}$ in northern Ukraine to trace levels of a few $\mu Bq \cdot m^{-3}$ or even within the usual background level in other European countries. Dispersion modeling determined the plume arrival time and was helpful in the assessment of the possible increase in airborne ^{137}Cs concentrations in Europe. Detections of airborne ^{90}Sr (emission estimate 345 – 612 GBq) and Pu (up to 75 GBq, mostly ^{241}Pu) were reported from the CEZ. Americium-241 represented only 1.4% of the total source term corresponding to the studied anthropogenic radionuclides but would have contributed up to 80% of the inhalation dose.

Synopsis

Wildfires in highly radioactive environment can re-emit radionuclides into the atmosphere. Such emissions present a potential health risk for firefighters.

Introduction

As a result of global fallout from atmospheric nuclear explosions and the Chernobyl nuclear accident, the Eurasian boreal forest represents one of the greatest stocks of long-lived anthropogenic radionuclides in the terrestrial environment, primarily ^{137}Cs ($T_{1/2}$ = 30.1 yr.).[1] Since large wildfires in 1992, the fire hazard in the Chernobyl area has been viewed with serious concern.[2] These fire events are capable of emitting radionuclides (RN) into the atmosphere and can redistribute part of the already deposited RN.[3] These RN are found in topsoil layers, forest litter, and in the biomass. Emission of natural RN such as ^{210}Po are also known to occur from wildfire events.[4, 5] Wildfires in heavily contaminated areas generate radioactive smoke particles and thus an additional radiation exposure through inhalation or ingestion of contaminated foodstuff, following RN re-deposition.[6] The consequences of wildfires in the highly contaminated area around the CNPP (parts of northern Ukraine, southern Belarus and the western part of the Russian Federation) as well as emission factors or resuspension factors have already been investigated at a local

level.[7-12] Evidence for long-range transport of RN from fires on an international scale is more recent.[1, 13] Considerable efforts have been made by Ukraine, Belarus, and the Russian Federation to limit the consequences of fires in contaminated areas.[14, 15] However, despite preventative measures (e.g., controled fires, fire-breaks, access trails, limitation of fuel quantities in some areas, minimization of human presence) intended to limit both ignition and the spread of wildfires, they occur on a yearly basis in the Chernobyl area[16, 17] and affect wildlife.[18] The Chernobyl ecosystem has regularly suffered from major wildfires notably in 1992, 1999, 2000, 2002-2004, 2006, 2010, 2015, 2016, and 2018 [15, 19] with major impacts on the vegetation cover.[20] For a brief historic review of wildfires in contaminated areas, see the Supporting Information (SI).

Herein, we investigate the devastating April 2020 wildfires, which lasted for about four weeks in the Ukrainian part of the contaminated areas around the CNPP. The detailed geographic analysis and timeline is provided in the SI. The fire situation in the CEZ and bordering areas was characterized by a combination of numerous ignitions and subsequent spread of fires. Their magnitude varied according to different parameters: 1) biomass type, vegetation density, and location accessibility (forest, meadow, peatland, and marshland); 2) meteorological parameters (wind speed, wind direction, precipitation frequency and amount). These multiple factors hindered firefighting, despite the mobilization of nearly 400 firefighters and 90 specialized aerial and terrestrial vehicles (two AN-32P airplanes, one Mi-8 water-bombing helicopter, heavy engineering equipment, and seven additional road construction machines of the Armed Forces of Ukraine). The first three weeks of April saw the development of particularly large and numerous fires. Two main fire areas were identified during this period: in the Polisske district and in the Kopachi-Chistogalovka-CNPP cooling pond (<12 km from CNPP). Daily information about burned areas including vegetation cover, contamination density, and radionuclide emissions were then published by the Ukrainian Hydrometeorological Institute (UHMI).[21] According to the UHMI, 870 km^2 were burned in total, including 65 km^2 in proximity to the CNPP and 20 km^2 on the left bank of the Pripyat river.

Because of a period of easterly and southerly winds, slight increases in the airborne ^{137}Cs were observed at a few western European locations while most of the airborne ^{137}Cs concentrations remained within the $\mu Bq \cdot m^{-3}$ range on a weekly sampling basis, which corresponds to the usual background level. Such western detections are somewhat rare since the general air mass circulation is usually easterly. A similar situation had already occurred from the end of August to early September 2002 with a slight increase in airborne ^{137}Cs concentrations in the western European atmosphere.[22] The follow-up of the April 2020 wildfire situation was scrutinized on a daily basis by the UHMI,[21] and regularly commented by the SCK-CEN[23, 24] and the IRSN.[25-28] In total about 1,100 ^{137}Cs results were gathered throughout Europe including already published data from the International Monitoring System (IMS) in support to the Comprehensive Nuclear-

Test-Ban Treaty Organization.[23, 24] This collection, which also includes a hundred values for ^{90}Sr, ^{238}Pu and $^{239+240}Pu$ from Ukraine, corresponds to the most comprehensive available dataset related to that event (see Tables S6 and S7, SI). The purpose of this study is to investigate both the RNs source terms and the additional exposure to RNs for firefighters and inhabitants of Kiev. Part of these assessments are based on numerous measurements performed during this event and dispersion calculation. RNs that were not determined have been estimated based on RN ratios typical of the Chernobyl accident and ^{210}Po results obtained during other wildfires.

Background

Starting on April 26, 1986 and for a period of ten days, the Chernobyl accident released harmful quantities of radionuclides of I, Cs, Te, Sr, Pu, and others (see Table S1, SI). Some regions of Belarus, Ukraine and the Russian Federation were seriously affected by the radioactive fallout from the CNPP accident.[29] About 6 million ha of forest including 2.5 million ha in Ukraine were heavily contaminated. In the most contaminated regions following the accident the dominant forests were young or middle-aged pine and pine-hardwood stands, with a high fire risk.[8] The highest radionuclide deposition density occurred in the area surrounding the CNPP, in the so-called Chernobyl Exclusion Zone (CEZ) in Ukraine and in the Polesie State Radioecological Reserve (PER) in Belarus. The CEZ, initially about 30 km in radius around the CNPP was subsequently enlarged to an oblong area of 2,600 km^2 with a 439 km circumference. It is located approximately 100 km north of Kiev (see Figure S1, SI). The CEZ is mostly covered by forest where radionuclides are distributed between soil, forest litter, and vegetation. Between 57 and 79% of the total ^{137}Cs contamination is stored within the upper soil layer (0- 2 cm).[30] Only a few percent of the ^{137}Cs inventory is contained in the living biomass, where ^{137}Cs behaves like potassium, its chemical analogue. During fire events in forested areas, the main source of radioactive aerosols is the burning forest litter. In comparison, the trees affected by the fire emit minor amounts of ^{137}Cs and ^{90}Sr and only trace amounts of Pu isotopes and ^{144}Ce.[31, 32] More information about radionuclide apportionment in the terrestrial ecosystem and fire impact is provided in the SI.

Present day contamination is the result of radionuclides released during the accident with a medium or long radioactive half-life [^{137}Cs ($T_{1/2}$ = 30.07 yr.), ^{90}Sr ($T_{1/2}$ = 29.14 yr.), ^{238}Pu ($T_{1/2}$ = 87.76 yr.), ^{239}Pu ($T_{1/2}$ = 24.13 10^3 yr.), ^{240}Pu ($T_{1/2}$ = 6.57 10^3 yr.), ^{241}Pu ($T_{1/2}$ = 14.35 yr.) and those arising as decay products of them: ^{241}Am ($T_{1/2}$ = 432 yr., ^{237}Np ($T_{1/2}$ = 2.144 10^6 yr.)]. Conversely to ^{137}Cs which spread and deposited all over Europe, ^{90}Sr, and Pu isotopes as nuclear fuel debris were mainly deposited in Ukraine and Belarus.[33] Cesium-137 is the preferred RN used in forecasting the long-term radiological consequences after an

accidental release, because of its radiotoxicity, bioaccumulation, comparatively long half-life and straightforward measurement procedure.

Once forests become contaminated with radiocesium, any further significant redistribution is limited. Processes of small scale redistribution include resuspension, fire and erosion/runoff.[3] According to the International Atomic Energy Agency (IAEA), none of these processes are likely to result in any significant migration of radiocesium beyond the location of initial deposition.[34] The question of radionuclide redistribution may be a matter of interest for nearest adjacent areas that would have not been initially contaminated or with a much lower contamination of their ecosystem. This gives interest for radionuclide redistribution on a local scale and detection of trans-border fire plumes. Depending on the wildfire intensity, smoke plumes may reach atmospheric layers up to several kilometres above ground level and travel for thousands of kilometers[1], or be maintained in the atmosphere up to about 20 days.[35] Previous studies have already brought some reassuring general information:[36] Over already contaminated areas the additional contamination due to redistribution of artificial radionuclides by a fire remains low, about 1% of the previous inventory.[32] Thanks to atmospheric dispersion and buoyancy effects, a sharp decrease in the airborne concentration can be expected with distance (a dozen fold less at a distance of 100 m and thousands fold less at a distance of several kilometres from the fire line.[32, 37] Regarding the redistribution or loss of RNs from a burned area, it has been suggested that a wildfire outbreak might export at least 40% and up to 90% of the ^{137}Cs inventory.[7-12] In other words, this would mean that a fire could virtually "clean" an area from ^{137}Cs. Current and historical research does not in any way support this proposition.

In several studies, it has been tried to determine the proportion of radionuclides that can be emitted into the atmosphere from a zone with a given contamination density or emitted from burning material during a fire, either through a resuspension factor K (m^{-1}) or an emission factor E_f (%). A compilation of both parameters can be found in the SI. The UHMI calculated estimates of radionuclide emission into the atmosphere daily. Their estimates relied on detailed satellite observations of the extent of the fires and combined the specific contamination density of the burned areas, the vegetation type, and the specific radionuclide distribution in the ecosystem. For the April 2020 fire event, the UHMI used a ^{137}Cs emission factor of 5% because of the exceptional intensity of the crown fires. As of April 20, a total of 690 GBq of ^{137}Cs would have been released into the atmosphere.[21] The ^{137}Cs source term was later re-evaluated including emission from April 20 to 30, leading to a release between 600 and 860 GBq for the CEZ, as well as 60 to 85 GBq for the Zhytomyr region.[30] Additionally, 13.5 GBq of ^{90}Sr and 0.059 GBq of Pu isotopes were estimated by the UHMI to have been released during fires. Using a similar approach (satellite observations of fire spots, burned areas, emission factors), Evangeliou & Eckhardt estimated that 341 GBq of ^{137}Cs, 51 GBq of ^{90}Sr, 2 GBq of ^{238}Pu, 0.033 GBq of ^{239}Pu, 0.066 GBq of ^{240}Pu and 0.504 GBq of ^{241}Am were released between April 1 – 22, 2020.[38]

Plume detection in Ukraine

Plume detection was revealed by a 1,000 to 10,000-fold ^{137}Cs increase (i.e. up to a fraction of a $Bq \cdot m^{-3}$ in the CEZ and up to a fraction of a $mBq \cdot m^{-3}$ in the Kiev area) as compared to the usual ^{137}Cs average background levels of about 3.5 $mBq \cdot m^{-3}$ in the CEZ and 6 $\mu Bq \cdot m^{-3}$ in Kiev.[32] Levels in excess of critical threshold concentrations (i.e. a reference level of 0.21 $mBq \cdot m^{-3}$ for ^{137}Cs in Ukraine) were observed in proximity to fire lines, owing to wildfire magnitude. High airborne contamination values were observed due to the proximity of aerosol samplers with the fire lines (i.e. 42 $mBq \cdot m^{-3}$ on April 12 at the Korogodske forestry "square 11" station). An even higher ^{137}Cs value of 180 $mBq \cdot m^{-3}$ (0.18 $Bq \cdot m^{-3}$) was momentarily reported on April 13 at the CNPP "Ukrenergomontazh - Open SwitchGear-750 point", at about 500 m from the damaged reactor. Such orders of magnitude were similar to those reported during previous wildfire outbreaks: 250 $mBq \cdot m^{-3}$ at the end of June, 2015 near the abandoned village of Polis'ke, 150 $mBq \cdot m^{-3}$ on July 29, 2016 in the "Red forest", 25 $mBq \cdot m^{-3}$ on June 29, 2017 in the CEZ, too.[39, 40] During the April 2020 fires, the UHMI estimated that the additional ground surface ^{137}Cs deposition in the CEZ peaked at about 65 $Bq \cdot m^{-2}$ where the surface contamination was already in the $MBq \cdot m^{-2}$ to the tens of $MBq \cdot m^{-2}$ range (pers. comm., O. Voitsekhovych, UHMI).

Strontium-90 was also detected in up to 20 locations, all of them in the highly contaminated area (see Table S7, SI). Based on about 40 pairs of ^{137}Cs and ^{90}Sr measurements, the $^{90}Sr/^{137}Cs$ activity ratio exhibited such a significant variation (0.04 – 6.67) that it could not reasonably be represented by an aggregated statistic (average value of 0.91). Hereafter, the highest ratio (6.67) was considered as an outlier and hence not taken into account as representative of the whole fire situation. It corresponded to the pair of ^{137}Cs and ^{90}Sr values that were by far the highest (as reported on April 13 from the OSG-750 station with ^{137}Cs=180 $mBq \cdot m^{-3}$ and ^{90}Sr=1,200 $mBq \cdot m^{-3}$) and because these concentrations were obtained over a very short period of time (~half an hour). 80% of the $^{90}Sr/^{137}Cs$ ratios were less than or equal to 1. Inversely, 20% of airborne ^{90}Sr concentrations were higher than ^{137}Cs. This suggests that ^{90}Sr and ^{137}Cs biomass contamination levels and magnitude of the fires were much more likely to be of significance in the observed $^{90}Sr/^{137}Cs$ ratio. Measurements performed using aerosol impactors (Yoschenko et al.) showed in general that ^{90}Sr bound to coarse particles with an activity median aerodynamic diameter (AMAD) of > 25 μm, while ^{137}Cs predominantly bound to the finer aerosol fraction.[32] Therefore, it is likely that the largest part of ^{90}Sr emissions remained airborne for only 1 – 2 km. The distance between mobile aerosol sampling units and the fire line thus participated to the variability of the $^{90}Sr/^{137}Cs$ ratio.

Contrarily to ^{90}Sr which behaves like calcium (a factor of main influence on the plant physiology), ^{137}Cs is much less bioaccumulated in wood .[18] Recently, Holiaka et al.[41] have reported a rather constant average ^{90}Sr

/^{137}Cs ratio of about 2.5 in wood disks of Scots Pine stems sampled approximately 5 km north of the CNPP. This value is clearly different from that found on average in aerosols (0.76, range 0.04 – 3.1) during the April wildfires. However, when looking into detail to the radial distribution of ^{137}Cs and ^{90}Sr in the wood disks the authors concluded that, due to the year-by-year root uptake increase, a newly formed annual ring receives a bigger amount of radiocesium than a ring formed in the previous years. In addition, ^{137}Cs is also translocated into these rings from older sapwood.[41] Conversely, the radial distribution of ^{90}Sr shows decreasing concentrations from heartwood to sapwood, i.e. decreasing ^{90}Sr concentrations from inner to outer parts.[41] The lower ^{90}Sr /^{137}Cs ratio observed in aerosols could thus be consistent with a partial combustion of aged tree trunks which remain charred after the fire goes through while the outer parts of the tree (peripheral annual rings with a lower ^{90}Sr /^{137}Cs ratio) are burned.

In addition to ^{137}Cs and ^{90}Sr, about thirty measurements for both airborne ^{238}Pu and $^{239+240}$Pu were reported from the CEZ (see Table S7, SI). Maximum values for hourly measurements reached 180 µBq·m^{-3} for ^{238}Pu and 450 µBq·m^{-3} for $^{239+240}$Pu on April 12 at the Korohodske forestry monitoring station. The average ^{238}Pu/$^{239+240}$Pu ratio found was 0.40, which is slightly lower than the value of 0.48 - 0.50 reported during the Chernobyl accident in 1986 or 0.47 found by Kashparov et al. [42-44] for the residual contamination of the environment in 2000. The ^{238}Pu/^{137}Cs, $^{239+240}$Pu/^{137}Cs and ^{238}Pu/$^{239+240}$Pu relationships shown in Figure 1 are those that will be used hereafter in source term assessments.

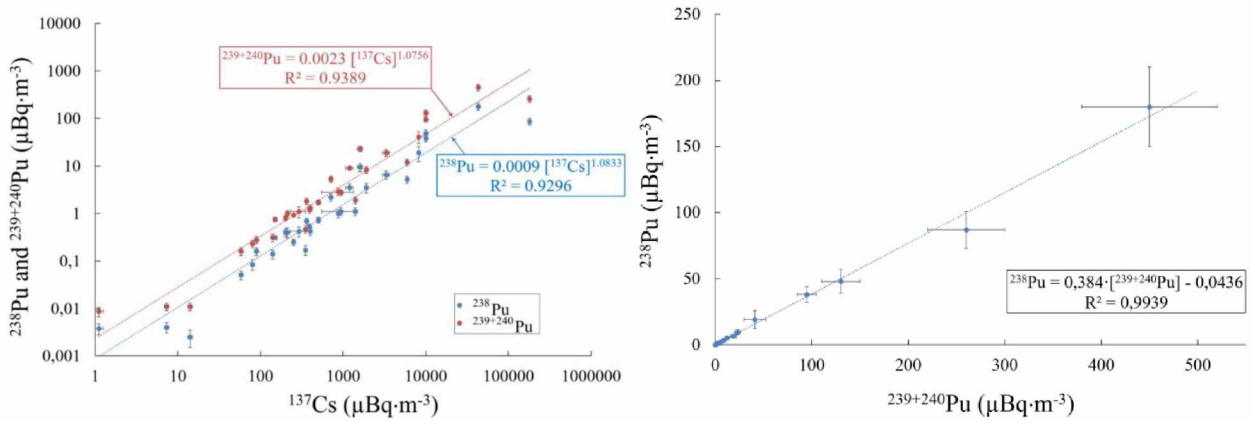

Figure 1: (Left) Airborne ^{238}Pu and $^{239+240}$Pu vs. ^{137}Cs concentrations in the CEZ, Ukraine, April 2020. (Right) Airborne ^{238}Pu concentration vs. $^{239+240}$Pu concentration in aerosols sampled in the CEZ, April 2020.

Except close to the fire spreading in the CEZ where the gamma dose equivalent rate was in the 0.5 - 30 µSv·h^{-1} range, the highest airborne concentrations measured elsewhere in Ukraine were not high enough to significantly increase the ambient gamma dose equivalent rate. Daily average airborne ^{137}Cs concentrations measured by the UHMI in Kiev reached 290 µBq·m^{-3} from April 8 to 9 and up to 700 µBq·m^{-3}

from April 10 to 11. The maximum observed average value during each daily sampling period remained far below the National Radiation Safety Standards of Ukraine[45] establishing the allowed concentration of ^{137}Cs to 800 $mBq \cdot m^{-3}$. Such concentration increases were concomitant with the smoke plume arrival in Kiev and have to be compared with the yearly average local background concentration of 6 $\mu Bq \cdot m^{-3}$ (usual range 3 – 8 $\mu Bq \cdot m^{-3}$).

Plume detection outside Ukraine

All the positive airborne ^{137}Cs measurements outside Ukraine during April 2020 were in the $\mu Bq \cdot m^{-3}$ range, i.e. within or just above the typical background ^{137}Cs level usually observed in the springtime (see Table S6, SI). The reason for this background and the low-level airborne ^{137}Cs persistence is examined in the Supporting Information. Considering the airborne ^{137}Cs background routinely observed and resulting from resuspension on a local scale, it was difficult to assert if the measured concentrations in april 2020 included a tiny and remote fire contribution. For instance, a weekly average value of 5.67 ± 0.58 $\mu Bq \cdot m^{-3}$ was observed at Seehausen in north-eastern Germany (52.891 N ; 11.729 E). This value is significantly higher than the airborne level in the westernmost Europe. However, it remains in the usual range of variability as a result of a comparatively more significant local Chernobyl deposition in 1986. In addition, Seehausen is also known for ^{137}Cs resuspension during periods of dry meteorological conditions (Pers. Comm. A. Dalheimer, DWD). Moreover, dispersion calculation did not reveal a noticeable transportation of airborne ^{137}Cs to Germany. It means that this location was not affected by the fire plume. In Norway, positive ^{137}Cs detections were observed at the two northernmost sampling locations (Viksjofjell, 69.62 N ; 30.72 E) and Svanhovd (69.45 N ; 30.04 E) with very low ^{137}Cs concentrations (< 1 $\mu Bq \cdot m^{-3}$). However, because of a persistent snow cover prone to prevent ^{137}Cs resuspension from soil both on a local and regional scales, it can be stated that airborne ^{137}Cs were mostly related to forest fires in Ukraine, as suggested by the coincidence between simulation of plume arrival and sampling dates with higher than usual airborne ^{137}Cs concentration (see *Plume dispersion analysis* section). Contrarily to what was first expected, in Eastern Europe and relatively close to Ukraine, the fire plume, although more concentrated than in Western Europe, did not ensue a significant ^{137}Cs increase above the usual local or regional ^{137}Cs background level which is usually also higher than in Western Europe. At some Eastern Europe locations, the weekly average ^{137}Cs activity may have hidden the peak value that would have been found if the sampling period had coincided with the sampling duration. In such case, the atmospheric dispersion modeling is the only way to retrieve this information (see *Plume dispersion analysis* section). For instance, in Budapest, it is estimated that the smoke plume arrived between April 5 and 6 and remained until April 9. A ^{137}Cs peak value of about 25 $\mu Bq \cdot m^{-3}$ was assessed. This peak cannot be foresee based on the weekly-average sampling value (12.8 $\mu Bq \cdot m^{-3}$). In Poland, the estimated ^{137}Cs peak value was about 50 $\mu Bq \cdot m^{-3}$ while the corresponding

weekly average value was at most about 6 $\mu Bq \cdot m^{-3}$ which is not much higher than the usual ^{137}Cs background level ranging from less than 1 $\mu Bq \cdot m^{-3}$ to a few $\mu Bq \cdot m^{-3}$.

In France, the maximum weekly ^{137}Cs activity level reached 1.31 ± 0.24 $\mu Bq \cdot m^{-3}$ from April 6 to 14, 2020 and was observed in the southeastern corner. It confirms model forecasts indicating that the highest value occurred in that region during this period. The weekly average ^{137}Cs value measured during the fire event was thus 4 to 8 fold higher than the ^{137}Cs background level in SE of France. The IRSN estimated that the average ^{137}Cs level added by fires in Ukraine during the presence of the air mass in France was at most 2 $\mu Bq\ m^{-3}$ which is of no health concern for the public. For that purpose, the average regional background ^{137}Cs level (0.15 to 0.30 $\mu Bq \cdot m^{-3}$) determined in a period ranging from March 15 to May 15 over the past 5 years was removed for the remaining sampling period. Finally, the amount of ^{137}Cs corresponding to the presence of the smoke plume was divided by the air volume filtered during its estimated presence. The concentration of airborne ^{137}Cs measured in France in April 2020 had not been observed since 2002 (from the end of August to the end of September 2002) when airborne ^{137}Cs concentrations increased up to 3.5 $\mu Bq \cdot m^{-3}$. This increase also resulted from wildfires raging in the Chernobyl area when for short periods the usual prevailing westerly wind was not in place. Winds were in fact easterly during Week 36 and Week 38, 2002, leading to twin spikes in the concentration of airborne ^{137}Cs in France, Germany, Czech Republic, and Austria. Outside the Chernobyl area, the highest airborne ^{137}Cs activity level was measured in Vilnius, Lithuania with up to 196 $\mu Bq \cdot m^{-3}$ during Week 36, 2002.[13] At that time, there were also a lot of fires in the vicinity of Vilnius,[46] which were responsible for an increase in PM_{10} up to 370 $\mu g \cdot m^{-3}$. Due to a higher water-soluble ^{137}Cs percentage, Lujaniene et al. (*2006*) concluded that these particulate matters were transported to Lithuania from forest fires occurring in Ukraine and Belarus.[13] Rising ^{137}Cs activity concentrations from smoke are due to both the enhancement of the airborne dust load, acting as ^{137}Cs carrier, but also to the fact that smoke is significantly rich in ^{137}Cs.[31]

We took the opportunity of this event to check if other radionuclides emitted into the atmosphere by wildfires might be used, in combination with ^{137}Cs, as a tool to attest the contribution of the wildfire plume far from the Chernobyl area. Strontium-90, plutonium isotopes, and ^{241}Am might be candidates. However, their tedious radiochemistry complicates their determination and their much lower expected airborne concentrations as compared to ^{137}Cs usually requires to gather together several weekly filters to exceed the detection limit in the composite sample. These RN are thus difficult to quantify above detection limits on a weekly aerosol-sampling basis. Looking for a more convenient-to-measure radionuclide whose activity ratio with ^{137}Cs might be relevant for wildfire plume detection at long distances, we also examined the airborne ^{40}K concentrations (See SI).

Source term assessment methodology

The UHMI performed RN source terms assessment based on environmental parameters such as satellite observations of burned areas, biomass density, and contamination density maps. Another way to assess radionuclide amounts emitted from the burned areas is to apply inverse modeling techniques combining atmospheric transport model and observed airborne concentrations. Such methodology was implemented using the comprehensive airborne ^{137}Cs dataset acquired on the European scale (see Table S6, SI) to estimate first the amounts of ^{137}Cs emitted into the atmosphere between April 2 and April 24, 2020. The method is described in the SI. Twenty-two different daily releases were estimated by inverse modeling between April 2 and 24, 2020. Although satellite images after April 24 indicate a persistent residual fire, releases were assumed insignificant after that date. In addition, the available measurements after April 24 are clearly not sufficient for an inverse modeling estimation of the source term. Our inverse modelling is based on a variational approach which consists in the minimization of a least-squares cost function assuming log-normal observations errors and wihout considering any additional background term (see SI). Performing Monte-Carlo simulations, 15,000 different source terms were computed in order to take into account uncertainties resulting both from dispersion modeling, meteorological fields and representation errors of observations. For instance, this analysis indicates that the estimated ^{137}Cs source term for the entire fire period lies between 700 and 1,200 GBq. This range reflects the set of all the above mentioned uncertainties. From April 2 to 15, our results indicate daily ^{137}Cs emissions ranging from 10 to 138 GBq (Figure 2). For this period, the source term estimation proves to be fairly robust since the sensitivity to observation perturbations is weak. The large number of observed values considered in the inverse modeling process reasonably explains the standard deviation on daily release rates remaining low. From April 15, the magnitude of the daily release rates varied significantly. The maximum daily release rate reached 362 GBq on April 16 and 241 GBq on April 20 thus corresponding to the highest releases estimated during the entire fire period. However, the standard deviations calculated for April 16 and 19 are large. This increases the source term margin of error and leads to a higher level of uncertainty.

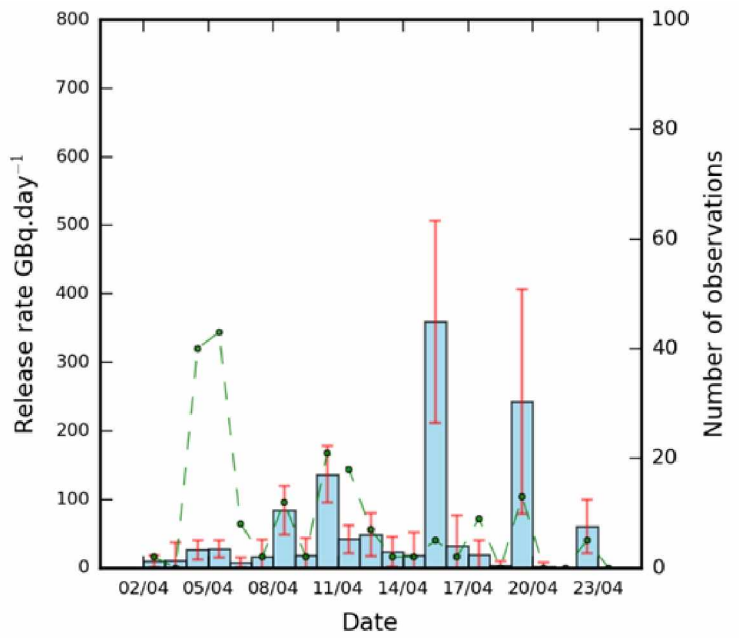

Figure 2: April 2 to 24 ^{137}Cs average daily release rates reconstructed by Monte Carlo analysis using n= 15,000 samples (blue rectangles) and the associated standard deviations (orange bars). The green dashed line represents the number of observations used for each daily release assessed by inverse modeling.

Plume dispersion analysis

The video of the plume dispersion simulation is available in the SI. An average source term was deduced from the Monte Carlo analysis as an input parameter. The smoke plume first went in the direction of the Russian Federation between April 2 and 3. From April 3 to 5, it moved to the south of Ukraine (including the Kiev region). From April 5 to 7, the plume continued to move towards both the west and south. It reached Romania, Hungary, the Czech Republic, eastern Poland, Austria and Slovenia during this period. The simulated hourly ^{137}Cs concentrations are about 10 - 50 µBq·m^{-3}, sometimes higher in eastern Romania and much lower to the west. From April 7, according to the model, there were very low ^{137}Cs concentrations (just above 1 µBq·m^{-3}) in southern Germany, France and Italy. These levels are close to the detection limits (DL). The model provides an explanation as to why the vast majority of sampling stations located in this geographical area did not report any concentration higher than DL. Furthermore, even in the case of a measurement > DL, as for instance in Austria and Poland, these measurements did not vary from the usual seasonal values. Modeling still tends to emphasize a contribution in ^{137}Cs concentrations from the fire, especially in the Czech Republic, Austria, Italy, Slovenia and France. Between April 8 and 10, a new plume reached the south of Ukraine again. The plume extended to Greece as of April 11. The hourly-simulated concentration reached up to 100 µBq·m^{-3} in the Thessaloniki area.

306 This estimate is fully consistent with measurements performed in Thessaloniki between April 11 and 13
307 with an average concentration of 25.5 $\mu Bq \cdot m^{-3}$ and a residence time of 3.5 ± 0.2 d.[47]
308 The wind direction changed again between April 12 and 13. Consequently, the wind blew towards Russia.
309 This change in direction corresponded to the most significant release period when the hourly simulated
310 concentrations exceeded 100 $\mu Bq \cdot m^{-3}$ at the IMS Russian station in Dubna. The plume then moved
311 northwest, to the northernmost part of Norway. The simulation shows hourly values up to 30 $\mu Bq \cdot m^{-3}$ over
312 this area on April 14. The plume passed through this region relatively quickly, in about a few hours. This
313 explains why the weekly sampling carried out in Svanhovd showed little variation compared to weekly
314 averages with a concentration of only 0.5 $\mu Bq \cdot m^{-3}$. This value is likely the result of fires being controlled.
315 During this period, very low weekly average ^{137}Cs concentrations were reported in Western Europe (about
316 1 $\mu Bq \cdot m^{-3}$). From April 15 to 19, the wind mainly blew east and southeast. Several slightly contaminated
317 air masses mainly affected the Kiev region and the more southern regions of Ukraine. On April 21, the
318 plume reached Greece again. The simulation consistently matched measurements carried out in Thessaloniki
319 (9.6 ± 0.8 $\mu Bq \cdot m^{-3}$) on April 21 with an estimated residence time of 11 ± 3 d.[47]
320 55% of the simulated ^{137}Cs concentrations were within a factor of 2 compared to the observed concentrations
321 (see Table S5, SI). This score provides significant validation of the reconstructed source term (see SI).
322 Maximum simulated and observed ^{137}Cs concentrations are compared from April 2 to 24 (Figure 3). The
323 observed and simulated ^{137}Cs maximum concentrations (maps A and B) are very similar. The maximum
324 simulated concentrations in Ukraine, Belarus and the Russian Federation are the highest and are consistent
325 with the maximum concentration levels reported in these countries. Further west, the correlation between
326 simulated and observed concentrations is also satisfactory, although the model tends to underestimate the
327 maximum observed concentrations in Austria. In any case, the maximum concentrations measured in this
328 area are low and the usual ^{137}Cs background level would have to be rigorously taken into account, if known,
329 in order to make a proper comparison between observed concentrations and simulated concentrations added
330 by the plumes. As a result of the agreement between simulations and observations, the hourly maximum
331 simulated ^{137}Cs concentration was derived at each sampling location (Figure 3, map C). Due to the spatial
332 resolution of the long-range dispersion model, values obtained at less than 50 km from the CNPP were not
333 taken into account because of the significant associated uncertainties. The maximum hourly concentrations
334 simulated in Eastern Ukraine, the western part of the Russian Federation and southern Belarus were above
335 1 $mBq \cdot m^{-3}$ (Figure 3, map C). Simulated concentrations then gradually decreased to the west. They were
336 above 10 $\mu Bq \cdot m^{-3}$ over a central band stretching from northern Norway to southern Greece. Further west,
337 concentrations were even lower but still above 1 $\mu Bq \cdot m^{-3}$ in southern France, Switzerland, western Austria
338 and Germany. This confirms that the ^{137}Cs concentrations measured in these countries were partly due to
339 the influence of the remote fire despite values being very close to observed seasonal measurements.

However, in Belgium and in the Netherlands, unusual ^{137}Cs concentrations (5.3 and 1.59 µBq·m^{-3}, respectively) were locally reported, that both our dispersion simulation and that of SCK-CEN cannot reproduce. It has been suggested that a local/regional simultaneous resuspension event might be the reason of the discrepancies between modeling and observations.

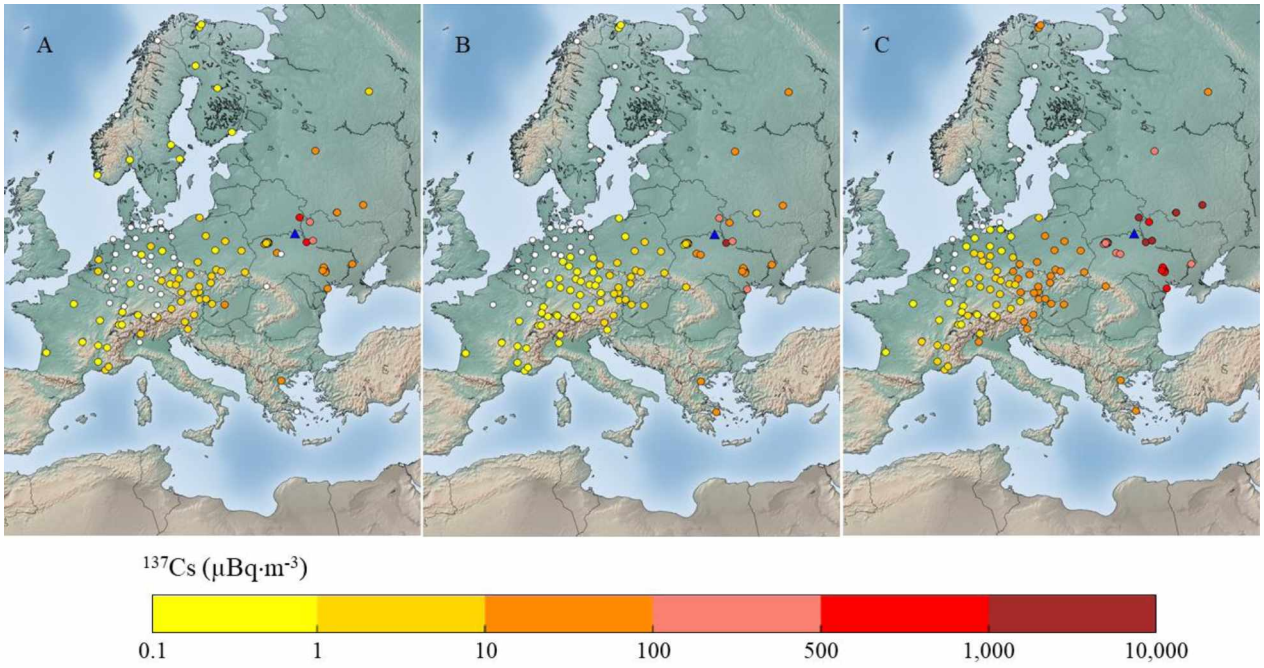

Figure 3: ^{137}Cs airborne concentration maps (µBq·m^{-3}) over the course of the April, 2020 wildfire event in Ukraine. (A) Maximum observed concentrations; (B) Maximum simulated concentrations; (C) Maximum values based on hourly simulated concentrations (i.e. maximum time-resolved peak concentrations). The same color scale applies to all maps.

According to Figure 4, the plume passed through Ukraine several times. At the Baryshivka station, hourly simulated concentrations exceeded 1 mBq·m^{-3} between April 17 and 20. In Greece, fire plumes reached the Thessaloniki area (northern Greece) on three occasions. The most significant episode around April 13 in this area was characterized by hourly simulated concentrations up to 100 µBq·m^{-3}. The average ^{137}Cs estimated concentration over the air sampling period (20 to 30 µBq·m^{-3}) remains consistent with measurement taken in Thessaloniki (25.5 µBq·m^{-3}). Further south, in Athens, no observable ^{137}Cs activity concentration (> 3 µBq·m^{-3}) was determined on three consecutive filters sampled from April 3 – 15. The geographical extent of the plume was very large as it reached as far as the northernmost part of Norway for a few hours on April 15 with a peak

simulated concentration of about 20 µBq·m^{-3} in Svanhovd. However, as the plume passed very quickly the concentration evaluated between April 14 and 20 remained below 1 µBq·m^{-3}, which is consistent with locally reported measurements. Further west, in Bialystok (Poland), Budapest (Hungary) and Bouc-Bel-Air (south of France), the simulation matched observation though the simulation underestimated values slightly. This discrepancy can be explained by the contribution of the usual ^{137}Cs background which represents a significant part of the total airborne concentration, especially when it is low, as is the case in France and to a lesser extent in Poland. According to the simulation, two plumes reached southeastern France between April 2 and April 24. The first plume, characterized by very low concentrations (estimated 2 to 3 µBq·m^{-3}), reached this region between April 8 and 15. A second plume arrived in Bouc-Bel-Air between April 23 and 29, but its magnitude remains imprecise due to the higher uncertainty resulting from the source term reconstructed during this time lapse. Comparisons at other European locations are provided in the SI (see Figure S7, SI). Dates and times of maximum simulated ^{137}Cs concentrations are also tabulated in the SI.

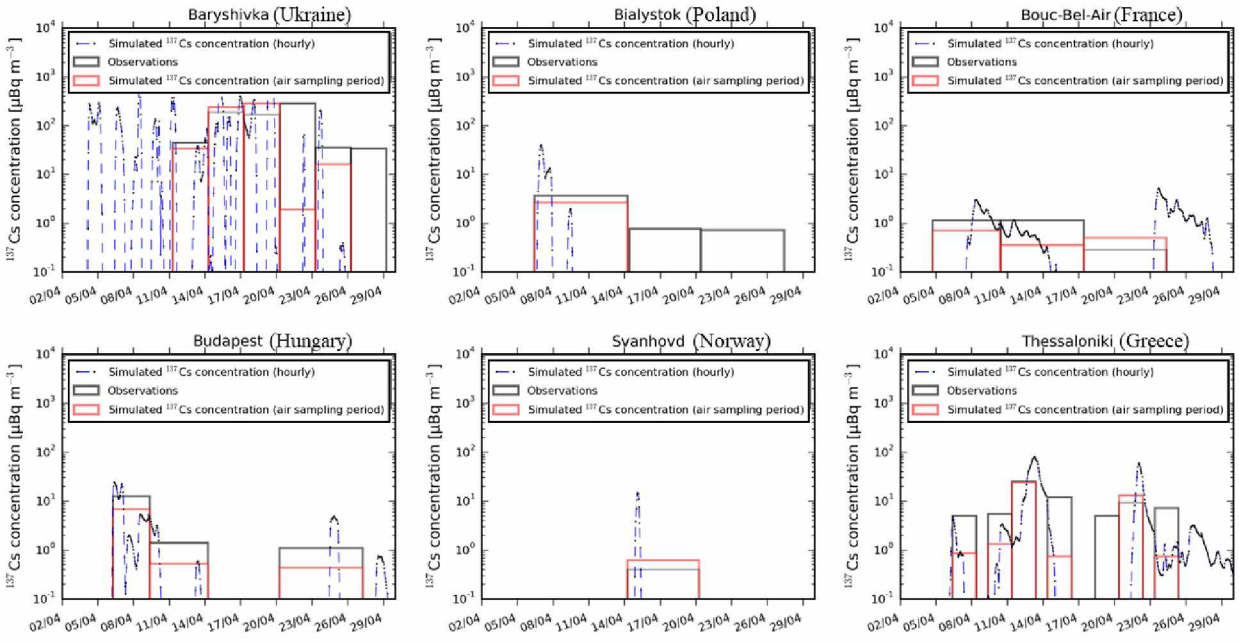

Figure 4: Example of comparisons between simulated and observed airborne ^{137}Cs concentrations at several European locations. The grey line shows the observed concentrations for each sampling period and the red line the simulated concentrations. The blue dashed line represents the simulated hourly concentrations.

^{90}Sr, ^{238}Pu, $^{239+240}Pu$ emissions

Because of the facility researchers have measuring ^{137}Cs at trace levels using γ-spectrometry, most investigations and reported data during this event focused on airborne ^{137}Cs as a tracer of biomass burnings, both on a nation-wide scale (i.e. in Ukraine) and on a continental scale. However, owing to their respective dose coefficients, there is much concern about the emission by wildfires of radionuclides such as ^{90}Sr, Pu isotopes, and ^{241}Am. Strontium-90 as well as ^{238}Pu and $^{239+240}Pu$ were measured only inside the CEZ but not on a wider scale. This prevented the use of the inverse methodology described for ^{137}Cs to assess: 1) the corresponding source terms 2) resulting airborne concentrations elsewhere in Ukraine and in the rest of Europe and 3) internal exposure. In France, all the filters taken at sampling stations that were assumed to be in the path of the fire plume according to the dispersion analysis, in addition to a slightly higher observed ^{137}Cs concentration than normal, were gathered in a composite sample representing 365,775 m^3. The following analyses were performed on this composite sample: α-spectrometry (^{238}Pu, $^{239+240}Pu$, ^{241}Am), ICP-MS (^{239}Pu and ^{240}Pu separately), proportional couting (^{90}Sr). Results for ^{238}Pu (0.12 ± 0.07 $nBq \cdot m^{-3}$) and $^{239+240}Pu$ (3.43 ± 1.09 $nBq \cdot m^{-3}$) were in the usual background ranges reported in France over the last decade ($0.03 - 0.42$ $nBq \cdot m^{-3}$ for ^{238}Pu and $0.10 - 2.85$ $nBq \cdot m^{-3}$ for $^{239+240}Pu$). Stontium-90 remained below a decision threshold of 62 $nBq \cdot m^{-3}$. As previously mentioned (see section *Plume detection in Ukraine*), emitted ^{90}Sr bound in general to the coarse aerosol fraction and is found to travel only short distances from a fire. Conversely, Yoschenko et al. demonstrated that transuranic elements which are in general bound to the fine aerosol fraction, are prone to travel much greater distances from the emission point.[32] Because of a high (60%) relative uncertainty associated to the ^{238}Pu result, the $^{238}Pu/^{239+240}Pu$ activity ratio observed in France was not appropriate to discriminate a possible Chernobyl signature. However, the $^{240}Pu/^{239}Pu$ mass ratio (0.25 ± 0.07) was slightly higher than the average value of 0.176 ± 0.03 usually observed in France during the last decade and which is typical of global fallout. Given the 0.41-0.42 typical signature of the Chernobyl fallout, this intermediate value could correspond to the added contribution following the smoke plume arrival in France in April.

To cope with the lack of large scale Sr and Pu results during this event we used the generally accepted Chernobyl-ratios between the above-mentioned radionuclides and airborne ^{137}Cs, and assumed these ratios to be representative of the emissions. Given the internuclide relationships derived from previous measured concentrations in the CEZ[48] and taking into account the previously estimated ^{137}Cs source term range (700 – 1,200 GBq), we considered the uncertainty associated with the relationships established between ^{90}Sr and ^{137}Cs on one hand and between $^{238, 239+240}Pu$ and ^{137}Cs on the other hand (Table 1).

Table 1: Estimations of Chernobyl-labelled radionuclides emissions (in GBq) during the April 2020 wildfires in Ukraine. Values for ^{137}Cs, ^{90}Sr, ^{238}Pu and $^{239+240}$Pu are derived from field measurements. Those for ^{239}Pu, ^{240}Pu, ^{241}Pu and ^{241}Am are deduced from typical activity or isotopic ratios characteristic of the Chernobyl accident. The grand total source term (^{137}Cs + ^{90}Sr + ^{238}Pu + ^{239}Pu + ^{240}Pu + ^{241}Pu + ^{241}Am) has been evaluated from values in bold characters.

Radionuclide		This study: Relationships used	This study: R^2 coef.	This study: Estimated emission range (GBq)	This study: Rounded average (GBq)	This study: Ratio to ^{137}Cs (%)	This study: % of total ST (%)	Other studies: Protsak et al. [21] (GBq)	Other studies: Tabachnyi et al. [30] (GBq)	Other studies: Talerko et al. [49] (GBq)	Other studies: De Meutter et al. [50] (GBq)	Other studies: Evangeliou et al. [38] (GBq)
^{137}Cs	(M)			**700 – 1,200**	**950**	100	62.2	690	660 – 945	574	220 -1,810	341
^{90}Sr	(M)	$^{90}Sr = 0.3313\ [^{137}Cs]^{1.061\pm0.030}$	0.8318	**346 – 613**	**480**	50.4	31.5	13.5	n.d.	n.d.	n.d.	51
^{238}Pu	(M)	$^{238}Pu = 0.0009\ [^{137}Cs]^{1.0833}$	0.9296	**1.1 – 1.9**	**1.5**	0.16	0.1	n.d.	n.d.	n.d.	n.d.	2
$^{239+240}$Pu	(M)	$^{239+240}Pu = 0.0023\ [^{137}Cs]^{1.0756}$	0.9389	**2.6 – 4.7**	**3.7**	0.39	0.2	n.d.	n.d.	n.d.	n.d.	0.099
^{238}Pu+$^{239+240}$Pu	(M)	$^{238,239+240}Pu = 0.0032\ [^{137}Cs]^{1.0771}$	0.9375	3.7 – 6.7	5.2	0.55	0.3	0.059	n.d.	n.d.	n.d.	2.1
^{239}Pu	(D)	$^{239}Pu/^{239+240}Pu = 0.403$ (*)		1.1 – 1.9	1.5	0.16	0.1	n.d.	n.d.	n.d.	n.d.	0.033
^{240}Pu	(D)	$^{240}Pu/^{239}Pu_{(activity)} = 1.496$ (**)		1.6 – 2.9	2.2	0.23	0.1	n.d.	n.d.	n.d.	n.d.	0.066
^{241}Pu (2020)	(D)	$^{241}Pu/^{239+240}Pu_{(activity)} = 19.1$		**50.5 – 90.1**	**70.3**	7.4	4.6	n.d.	n.d.	n.d.	n.d.	
^{241}Pu (2020)	(D)	$^{241}Pu/^{239}Pu_{(activity)} = 39.75$		42.3 – 75.6	59.0	6.2	3.9	n.d.	n.d.	n.d.	n.d.	n.d.
^{241}Am (2020)	(D)	$^{241}Am/^{241}Pu = 0.328$		**13.9 – 29.6**	**21.7**	2.3	1.4	n.d.	n.d.	n.d.	n.d.	0.504
^{137}Cs+^{90}Sr+ΣPu+^{241}Am				**1,114 – 1,939**	**1,530**		100					

(M): measured, (D): deduced, ST: Source Term, n.d.: not determined

(*) Values taken from ref.[48] for the organic layer of the surface soil (litter and humus).

(**) derived from the low-uncertainty ^{240}Pu /^{239}Pu (isotopic) ratio 0.408 ± 0.003 obtained by Muramatsu et al.[48] in the Chernobyl environment.

Our ^{137}Cs source term estimation is fully consistent with that proposed by Ukrainian researchers: 690 GBq as of April 20 or 660 to 945 GBq until the end of the blaze event.[21, 30] Theses estimates are based on a very different method combining land cover and vegetation features, radionuclide distribution in the ecosystem, biomass burning emission factors, and fire satellite detections. Evangeliou & Eckhardt indicated that their model underestimated measurements by about 70%, which means that in their study the average modeled concentration was almost half of the average measured concentration.[38] Based on observed airborne concentrations, our estimated average ^{90}Sr emission (480 GBq) is much higher than those estimated by Protsak et al. (13.5 GBq) and Evangeliou & Eckhardt (51 GBq). These two ^{90}Sr assessments combined estimations of the residual ^{90}Sr biomass contamination, satellite detections and used a ^{90}Sr emission factor of 0.2% (i.e. 25-fold lower than for ^{137}Cs, based on their research). Our ^{238}Pu estimate is also consistent with that of Evangeliou & Eckhardt.[38] However, the $^{238}Pu/^{239+240}Pu$ activity ratio (~20) indicated by these authors[38] represents a serious discrepancy and is inconsistent with the characteristic Chernobyl Pu isotopic signature of 0.48 or with the value of 0.47 typical of the residual contamination observed in 2000 in Ukraine.[42, 44] In our study, the relationship obtained beween ^{238}Pu and $^{239+240}Pu$ can be expressed by $^{238}Pu = 0.384[^{239+240}Pu]-0.0436$ ($R^2 = 0.9939$). The slope of the $^{238}Pu/^{239+240}Pu$ adjustement (0.384) fits the one characteristic of the Chernobyl accident (0.4 - 0.5).

^{239}Pu and ^{240}Pu emissions

Distinct determinations of ^{239}Pu and ^{240}Pu were not reported. Both Pu isotopes behave similarly in the environment and have a much longer half-life as compared with the period of time that went by since the accident, thus we can neglect their differential decay. We can assume that the $^{240}Pu/^{239}Pu$ ratio at the emission to be the same as in soil or in the biomass. Muramatsu et al. [48] indicated a relative consistency of the mass (or atom) ratio (average 0.408 ± 0.003, range 0.386 - 0.412) regardless of the $^{239+240}Pu$ concentrations range in surface soil samples (i.e. organic rich layers). In some moss and soil samples of Chernobyl, Jakopic et al.[51] reported mass ratios of 0.3624 ± 0.0011 and 0.4140 ± 0.0035, respectively. In forest soil, a mass ratio ranging from 0.186 to 0.348 was found.[52] We retain an average $^{240}Pu/^{239}Pu$ mass ratio of 0.41 which once expressed in $^{240}Pu/^{239}Pu$ activity ratio corresponds to a value of 1.50, close to the characteristic activity ratio (1.40) that can be deduced from the Chernobyl releases (see Table S1, SI). Plutonium-239 can also be expressed with reference to $^{239+240}Pu$ with a typical activity ratios ($^{239}Pu/^{239+240}Pu$) of 0.403.[48] Based on our $^{239+240}Pu$ emission estimate (2.6 – 4.7 GBq) we derived a ^{239}Pu emission between 1.1 and 1.9 GBq and a ^{240}Pu emission between 1.6 and 2.9 GBq.

^{241}Pu and ^{241}Am emissions

Unfortunately, for the sake of study, no ^{241}Pu or ^{241}Am determination was reported for that event. Plutonium-241 releases during the Chernobyl accident (~6 PBq) was the largest contributor to the total plutonium released amount (see Table S1, SI). Despite its rather short half-life ($T_{1/2}$ = 14.4 yr.), ^{241}Pu still denotes a significant reservoir of environmental radioactivity. However, as a pure β emitter (maximum energy of only 20.8 keV) ^{241}Pu represents a lesser radiological risk compared with other α-emitting plutonium isotopes (except via its decay product ^{241}Am). Since the Chernobyl accident, only 19.1% of the ^{241}Pu amount released in 1986 is still present in the environment. It is possible to assess the ^{241}Pu emission by the April 2020 wildfires using the original ^{241}Pu/$^{239+240}$Pu activity ratio and applying a simple ^{241}Pu decay. This ratio was estimated for May, 1986 in a range between 70 and 100.[43, 53-57] or even in a range of 82 to 120 in upper parts of lichens, 98 in air filter (May 1, 1986), 95 in grass (May 1, 1986).[56] Considering a global average ratio of 100 at the time of the accident and neglecting ^{239}Pu and ^{240}Pu decays as of April 2020, the ^{241}Pu/$^{239+240}$Pu activity ratio would have been about 19.1 during the wildfire event. Given the previously estimated $^{239+240}$Pu emission (2.6 – 4.7 GBq) results in a ^{241}Pu emission between 50.5 and 90.1 GBq. Another estimation of the ^{241}Pu emission can be performed using the initial ^{241}Pu/^{239}Pu mass ratio of 0.123 ± 0.007 (ref.[55]) for May 1986 and confirmed by the value of 0.0384 ± 0.0022 determined for 2009.[51] Once expressed in activity ratio and ^{241}Pu-decay corrected to date, the ^{241}Pu/^{239}Pu activity ratio is 39.75. Considering the above estimated ^{239}Pu emission range (1.1 – 1.9 GBq) leads to a ^{241}Pu emission ranging 42.3 – 75.6 GBq, consistent with the above-mentioned estimation based on the ^{241}Pu/$^{239+240}$Pu ratio (50.5 – 90.1 GBq).

Most radiological concern comes from ^{241}Am. This nuclide results from ^{241}Pu decay and is characterized by a much longer half-life ($T_{1/2}$ = 432.7 yr.), a much higher radiotoxicity (as an α-γ emitter), and a higher environmental mobility than its parent.[53] As a result, the in-growth of ^{241}Am from ^{241}Pu decay exhibits an increasing radiation risk with time. By 2058, the ^{241}Am activity will exceed that of plutonium isotopes by about a factor of two.[58] In addition, its inhalation effective dose coefficient is about 245 fold higher than for ^{241}Pu. A deeper insight into the differential soil-to-plant transfer of both Pu and Am is necessary to assess the ^{241}Am emission from that of ^{241}Pu. For both radionuclides, the downward migration in soil is expected in the same range (0.1 – 0.5 cm·yr^{-1}). However, a 1.5 fold higher migration velocity has been reported for ^{241}Am as compared with Pu in the Chernobyl-contaminated environment of Belarus characterized by sandy soil of various types (soddy podzolic sand, loamy sand and peat bog).[58] Despite a high variability induced by both plant species and soil structure and composition, both concentration factors (Cf_{Am} and Cf_{Pu}) between soil and plant (root uptake path) remain much lower (2 to 3 order of magnitude less) compared to ^{137}Cs and even more so to ^{90}Sr.[54, 58, 59] As a rule of thumb, the ^{241}Am soil-to-plant concentration factor (Cf_{Am}) exceeds that for Pu.[58, 60] Sokolik et al.[58] proposed an average Cf_{Am} to Cf_{Pu} ratio of 2.2 (1 – 6 range) for meadow grasses. Other determinations indicating a higher Cf_{Am} to Cf_{Pu} ratio were reported: about a factor of 2 in crops[61] and 2.3 (1.6 - 3.3 range) in bilberry and lingonberry plants.[59] Concentration factors from forest litter

485 to spruce and pine needles, to pine root and stem, to spruce bark, to fern, alder and heather have been
486 summarized in Mietelski et al.[54]with a similar average of 2.6 (0.3 - 5.7 range). Based on the above-mentioned
487 values and as a conservative approach, we considered hereafter a differential soil-to-plant transfer between
488 ^{241}Am and ^{241}Pu (Cf_{Am}/Cf_{Pu}) of 2.4. In the same period of time (34 yr.) since the Chernobyl accident, the
489 ingrown ^{241}Am represents 2.6% of the ^{241}Pu initially released. We can neglect the ingrowth of ^{241}Am stored
490 in the burnable biomass because 90% of the Pu is stored in the litter with a degradation rate of about a few
491 years.[32] As of April 2020 the theoretical activity ratio ^{241}Am/^{241}Pu from Chernobyl was thus about 13%.
492 Multiplying this ratio by the above-mentioned Cf_{Am}/Cf_{Pu} ratio of 2.4 leads to a ratio of 0.328 between the
493 amounts of ^{241}Am and remaining ^{241}Pu emitted into the atmosphere in April 2020. To cope with the lack of
494 experimental determination the same biomass burning emission factor (i.e. 1%) can safely be considered
495 for both RN since Pu and Am have a much higher boiling point as compared with the maximum expected
496 fire temperature. In such a case, their emission during wildfires is assumed to be mainly limited through the
497 uplift of ashes and not through the gas phase.[5, 62] The higher ^{241}Am release potential thus likely arises from
498 its higher upstream soil-to-plant transfer. The slightly higher ^{241}Am release potential than for Pu is validated
499 by the experimental determination of the resuspension factor by wildfires (K) (see Tables S2 and S3, SI).[62,
500 63] In short, given the overall range estimated for the ^{241}Pu emission (42.3 – 90.1 GBq) results in an ^{241}Am
501 emission estimation between 13.9 GBq (42.3 GBq x 0.328) and 29.6 GBq (90.1 GBq x 0.328).

502 The particular case of storage facility risks in the vicinity of the CNPP are detailed in the information notes
503 published by the IRSN.[25-28] The Ukrainian authorities indicated that the spent fuel storage facility N1 (which
504 contains spent fuel from the Chernobyl NPP decommissioned in 2000) was located in the immediate area
505 of the NPP, thus safe from the fires. The spent fuel storage facility N2 located in the CEZ contains empty
506 tanks made of huge reinforced concrete structures surrounded by a fence. The authorities also said that the
507 Pidlisne storage facility, made of fireproof reinforced concrete structures and used to store nuclear waste,
508 was also located in a place at low risk to fires. As a precaution, the forest was cut down around the storage
509 facility to avoid the threat of fire, and the distance from green spaces was more than 100 meters.[64] In addition
510 to waste managed in the industrial zone around the sarcophagus and engineered disposal sites, non-
511 engineered near-surface trench dumps were used as waste repositories. In the early 2000's, ^{241}Pu was
512 responsible for approximately 20% of the overall activity, while ^{241}Am and ^{238}Pu were responsible for 45%
513 and 15% of the total α-activity, respectively.[65] Considering the numerous waste disposal sites that contain
514 large amounts of radionuclides and that are in the immediate proximity to the CNPP, it is likely that their
515 radionuclide content was spared from fire as previously mentioned.[66] Indeed, their soil cover naturally
516 protects them. However, vegetation can grow in this soil, uptake radionuclides, and as a result, become
517 highly contaminated.[67] After the trenches were covered with soil, some of them were also planted with small
518 pine trees.[65] During the course of the trees' growth, partial uptake of the radionuclides buried in the trenches

519 occurs. These radionuclides are then distributed between the trees and the topsoil through litterfall. Waste
520 trenches are also periodically flooded by groundwater. As a result of a solution pH in the 4.8 – 5.1 range,
521 radionuclide dissolution of fuel particles and migration of the corresponding radionuclides can be more
522 effective in their proximity.[68] Thiry et al.[67] estimated that the maximum ^{90}Sr transfer will be reached 40
523 years after planting with 7% of the total ^{90}Sr content in the trench being transferred to the trees, and 12% to
524 the forest litter. According to the transfer calculation conducted by Thiry et al.[67] on waste buried (trenches),
525 the transfer of ^{90}Sr from soil to tree and litter has been estimated to be at most 7% and 12%, respectively
526 thus 19% for the burnable biomass. The ^{90}Sr transfer is thus 216 fold more efficient than that of ^{137}Cs,[67]
527 resulting in a maximum ^{137}Cs transfer of only 0.09%. Recent work by Kashparov et al. confirms that the
528 activity of the mobile form of ^{90}Sr in the trench has presently reached its maximum value.[69] This results
529 from the decrease of the amount of remaining nuclear fuel particles not yet dissolved in topsoil and the
530 reduction of the ^{90}Sr soil-to-plant transfer due to its radioactive decay. Regarding Pu, it can be emphasized
531 that, unlike ^{137}Cs and ^{90}Sr, the transfer of plutonium to plants is extremely low; this element is therefore
532 present at only trace amounts in forest organic matter and remains fixed in the mineral soil fraction
533 contaminated in 1986. Yoschenko et al. estimated that its transfer to trees plus litter was 3.5 fold lower than
534 for ^{137}Cs.[32] Using this ratio we can estimate a Pu concentration factor from soil to plant + litter burnable
535 biomass (Cf_{Pu}) of 0.026%. Taken this factor and considering the previously mentioned ratio Cf_{Am} / Cf_{Pu} of
536 2.4 results in a transfer factor for ^{241}Am (Cf_{Am}) of 0.0624%. In short, considering the biomass emission
537 factor of 4% (for ^{137}Cs and ^{90}Sr) and 1% (for Pu isotopes and ^{241}Am), the proportion of radionuclides emitted
538 into the atmosphere by the wildfires as compared to their trench content can be estimated at 0.036‰, 7.6‰,
539 0.0026‰ for ^{137}Cs, ^{90}Sr and Pu isotopes, respectively. The volume of waste in the replanted trenches is not
540 precisely known. The trenches are scattered over a total area of 450 ha in the CEZ (around 10^6 m^3).[65] A
541 more refined estimate of the potential radionuclide emissions could be performed based on the buried waste
542 amount and existing biomass on their surface. However, such specific estimates require further investigation
543 which is beyond the scope of this study.

544 **Dose assessment**

545 A dose assessment was performed on two categories of people: firefighters who took part in firefighting in
546 the CEZ and inhabitants of Kiev at about 100 km from the CEZ. Firefighters have already been identified
547 at risk in the event of a forest/bush fire over the dumps (storage trenches), as their occupational dose may
548 exceed the constraint of 0.3 mSv·yr^{-1}.[65] Their inhalation dose assessment was performed taking deliberately
549 a conservative approach with the followings assumptions: 1) the firefighters had no respiratory protection
550 (as part of Personal Protective Equipment, PPE) such as a self-contained breathing apparatus (SCBA) or a
551 facemask, 2) all aerosol sizes resulting from wildfires were belonging to the respirable fraction (<10 μm),

552 3) a total working time in the exclusion zone of a hundred hours for each of them (10 days with 10 working
553 hours per day), 4) a breathing rate of 3 $m^3 \cdot h^{-1}$ corresponding to a very heavy exercise.[70] The airborne
554 concentrations considered were based on field measurements where ^{137}Cs, ^{90}Sr, ^{238}Pu and $^{239+240}Pu$ were
555 simultaneously measured (see Table S7, SI). Detailed estimations for ^{239}Pu, ^{240}Pu, ^{241}Pu and ^{241}Am (both not
556 measured) were derived from measured ^{137}Cs concencentrations and Pu isotopic ratio according to the
557 relationships mentioned in Table 1. Two possibilities were considered for the measured values: maximum
558 observed or average values. The first assumption, leading to airborne concentrations of 1 $Bq \cdot m^{-3}$ (rounded
559 values) for both ^{137}Cs and ^{90}Sr, and 1 $mBq \cdot m^{-3}$ for ^{238}Pu, is very pessimistic since the highest measured
560 concentrations at similar orders of magnitude were only reported during short periods of time (i.e. peak
561 values over half an hour). Thus the consideration of such constant concentrations over a hundred-hour
562 exposure is likely excessive and must be considered as an upper limit that could not be exceeded. This led
563 to the following calculated airborne concentrations: 1 $mBq \cdot m^{-3}$ for ^{239}Pu, 1.5 $mBq \cdot m^{-3}$for ^{240}Pu, 44 $mBq \cdot m^{-3}$
564 for ^{241}Pu and 12 $mBq \cdot m^{-3}$ for ^{241}Am. Given the above-mentioned considerations and the effective dose
565 coefficients for workers (Table 2), the corresponding committed effective dose over an integration time of
566 50 years by inhalation of radioactive smoke at such RN concentrations would have reached 170 microSievert
567 (μSv) in total of which 80% comes from ^{241}Am (Table 3). A much more likely dose assessment even if may
568 be an underestimation can be established based on spatially averaged concentrations (Table 3). In this case,
569 the resulting dose induced by inhalation of all artificial RN considered in this study over a period of
570 100 hours would be 1.3 μSv. These estimated doses are much lower than the internationally accepted
571 maximum dose for the public from external sources (1 $mSv \cdot yr^{-1}$).
572
573 Table 2: Effective dose coefficients ($Sv \cdot Bq^{-1}$) of RN of interest for the general public (adult) and for
574 workers during wildfires.[71]

Radionuclide →	^{137}Cs	^{90}Sr	^{238}Pu, ^{239}Pu, ^{240}Pu	^{241}Pu	^{241}Am
Absorption type →	F	M	S	S	M
Dose coefficient ($Sv\ Bq^{-1}$) *Adult of the Public (*)*	$4.6\ 10^{-9}$	$3.6\ 10^{-8}$	$1.6\ 10^{-5}$	$1.7\ 10^{-7}$	$4.2\ 10^{-5}$
Dose coefficient ($Sv\ Bq^{-1}$) *Workers (*)*	$4.8\ 10^{-9}$	$3.6\ 10^{-8}$	$1.5\ 10^{-5}$	$1.6\ 10^{-7}$	$3.9\ 10^{-5}$

575 (*) aerosol diameter of 1 μm.
576 Notes: Absorption types: F = Fast, M = Moderate, S = Slow. For ^{90}Sr, the type M corresponding to fuel
577 fragments or when unspecified forms is recommended for the general public [72] and for workers [73] even if
578 there is no recommendation in [71]. For Pu isotopes a S-type solubility has been considered as a result of the
579 Pu oxide forms released during the Chernobyl accident.
580
581 Despite rather high airborne ^{137}Cs concentrations measured near fire lines, the low ^{137}Cs dose coefficient, as
582 compared with that of ^{90}Sr or Pu isotopes, minimizes its dose impact (only 1% of the total inhalation dose,
583 Table 3). It is important to point out that the ^{137}Cs dose coefficient is 10 fold less significant than that of ^{90}Sr

584 (Table 2). Since airborne ^{90}Sr concentrations were only 0.8 fold lower than those of ^{137}Cs on average, ^{90}Sr
585 resulted in a greater average dose impact. As α-emitters, ^{238}Pu, ^{239}Pu and ^{240}Pu do not cause any significant
586 external exposure. However, owing to their high radiotoxicity, the contribution of transuranic elements by
587 inhalation to the exposure of firefighters is not something to ignore. Airborne Pu concentrations in the
588 proximity of fire lines were about 250 fold lower than ^{137}Cs concentrations on average. But the Pu effective
589 dose coefficients are about 3,500 fold higher than that of ^{137}Cs. These significant differences in dose
590 coefficients make $^{238,239,240}Pu$ isotopes definitively more significant dose contributors. This is almost the
591 same for ^{241}Am which emits mostly high-energy α-particles in addition to low-energy γ-rays (E = 60 keV,
592 13%). Eventually, the highest inhalation dose coefficient among the studied RN belongs to ^{241}Am which has
593 a dose coefficient of about 250 fold higher than that of ^{241}Pu. In any case, the estimated effective dose for
594 firefighters (0.013 $\mu Sv \cdot h^{-1}$) as a result of inhalation of those radionuclides remained lower than or similar to
595 the external exposure to radiation from the highly contaminated environment of the CEZ which is most
596 often between 0.1 and 1 $\mu Sv \cdot h^{-1}$, and with maximum values about 10 $\mu Sv \cdot h^{-1}$. [6, 32] However, they may have
597 been significantly reduced (1 to 2 orders of magnitude) if protective equipment has been actually used.[6]
598
599 Table 3: Estimated effective doses (in μSv) by inhalation of artificial RN at a breathing rate of 3 $m^3 \cdot h^{-1}$ and
600 during 100 hours, for firefighters in the CEZ during the April 2020 wildfires, for two scenarios:
601 (A) observed peak concentrations, (B) spatially averaged concentrations.

Scenario	Radionuclide	^{137}Cs	^{90}Sr	^{238}Pu	^{239}Pu	^{240}Pu	^{241}Pu	^{241}Am	Total
A	Maximum airborne concentration ($mBq \cdot m^{-3}$)	1000	1000	1	1	1.5	44	12	
	Bq inhaled after 100 h	300	300	0.3	0.3	0.4	13.2	3.6	
	Dose (μSv)	1.44	10.8	4.5	4.2	6.3	2.1	141	170
B	Average airborne concentration ($mBq \cdot m^{-3}$)	10	10	0.01	0.007	0.01	0.3	0.09	
	Bq inhaled after 100 h	3	3	0.003	0.002	0.003	0.09	0.027	
	Dose (μSv)	0.014	0.108	0.045	0.029	0.042	0.014	1.05	1.3
	Contribution to the total inhalation dose	1.1%	8.3%	3.5%	2.2% 8,9%	3.2%	1.1%	80.6%	

602
603 The inhalation dose rate (0.013 $\mu Sv \cdot h^{-1}$) would have also remained about 8 fold lower than the average
604 ambient dose rate of 0.1 $\mu Sv \cdot h^{-1}$ from the natural background.[6] When considering maximum airborne
605 concentrations, the dose rate estimation (1.7 $\mu Sv \cdot h^{-1}$) by inhalation of artificial RN for firefighters is similar

606 to the order of magnitude of the external exposure dose rate from the highly contaminated environment (1
607 – 10 $\mu Sv \cdot h^{-1}$). It would have been 10 to 20 fold higher than the external ambient dose rate from natural
608 background radiation of 0.1 $\mu Sv \cdot h^{-1}$ (range 0.07 - 0.23 $\mu Sv \cdot h^{-1}$) and the internal dose of 0.18 $\mu Sv \cdot h^{-1}$ (range
609 0.05 - 1.3 $\mu Sv \cdot h^{-1}$), respectively.[6, 63] Our estimates are consistent with those from previous studies,[6, 62, 63]
610 which also indicate the predominant contribution of transuranic elements in the internal inhalation
611 exposure.[6] These studies also point out that the dose received by firefighters because of smoke inhalation
612 (internal dose) was only about 1% of the dose induced by ground shine and the effective external dose would
613 have exceeded the expected internal dose for firefighters even without protective equipment.[6] The dose of
614 external radiation from the smoke (cloud shine) in case of fire was not taken into account as it is negligible
615 (10^4 - 10^5 fold lower) as compared to the external dose (ground shine) from the contaminated environment.[32]

616 Chernobyl-labeled radionuclides aside, naturally occurring radionuclides with a high dose coefficient and
617 that are prone to emission during a wildfire have to be considered. This is typically the case for, among
618 others, ^{210}Po ($T_{1/2}$ = 138 d.) as a progeny of the relatively long-lived ^{210}Pb ($T_{1/2}$ = 22 yr.) and which
619 accumulates in the biomass through foliar uptake. Polonium-210 has an effective dose coefficient of 3.3
620 10^{-6} Sv/Bq and 3.0 10^{-6} Sv/Bq for an adult of the public and for a worker, respectively, and given a type M
621 solubility corresponding to chloride, hydroxide, volatilized Po and all unspecified Po forms. Polonium is
622 among the radioactive elements with a low fusion point (about 254 °C for elemental Po under 1 atm). The
623 volatilization points of common polonium compounds are about 390 °C thus much lower as compared to
624 mean wildfire temperatures (> 500 °C with maximum of 1,000 –1,200 °C).[5] As a result, ^{210}Po is easily
625 emitted during a fire. Carvalho et al. suggested that, as a result of combustion, a percentage of the ^{210}Po
626 initially in the biomass becomes concentrated in flying ash particles which corresponds to the refractory
627 remaining fraction after organic and water losses, while another percentage of the ^{210}Po forms gaseous ions
628 after volatilization which are likely to be captured by electrostatic forces onto smaller aerosol particles (<
629 0.5 µm), due to their higher surface/mass (or volume) ratio.[5] Because of its high dose coefficient these
630 processes are a further reason to take ^{210}Po into account when estimating internal exposure during a wildfire.
631 Carvalho et al. measured a maximum airborne ^{210}Po concentration of 70 $mBq \cdot m^{-3}$ in the proximity of a fire
632 line in Portugal in the summer 2012.[5] This concentration is as much as 1,000 fold higher as compared with
633 the airborne ^{210}Po background level of about a dozen $\mu Bq \cdot m^{-3}$ in the Northern hemisphere.[74] Since ^{210}Po was
634 not measured in April 2020, it is difficult to assert that such concentration would have been reached in the
635 CEZ even though wildfire conditions can be assumed to be similar. In order to adapt to the absence of ^{210}Po
636 measurement we propose to use a wider range of possible airborne ^{210}Po concentrations encompassing the
637 concentration found in Portugal, i.e. 1, 10 and 100 $mBq \cdot m^{-3}$, in order to provide the order of magnitude of
638 the inhalation dose assessment. We can estimate a maximum breathing rate at 3 $m^3 \cdot h^{-1}$ for a firefighter

working 10 hours a day (as established by Kashparov et al., 2015) during 10 days.[6] Based on a ^{210}Po concentration of 10 $mBq \cdot m^{-3}$, the inhalation dose would increase by 9 μSv. This would represent 5% of the inhalation dose from radionuclides originating from Chernobyl ($^{137}Cs + {}^{90}Sr + \Sigma Pu + Am$) when considering maximum airborne concentrations. When considering average airborne concentrations this would result in a 7 fold higher dose.

With the exception of the area in the immediate proximity to the fire, concentrations rapidly decreased and did not present any concern for public health. At greater distances from the blaze, as in Kiev, the airborne ^{137}Cs measured concentrations, or calculated concentrations for the other RN, remained between 1,000 and 10,000 fold lower on average than those in the CEZ and did not present any risk for the population, even when considering ingestion of foodstuffs subject to radionuclide deposition. To compute airborne RN concentrations for an inhabitant of Kiev, we used the previously calculated RN source terms (Table 1) as an input parameter in the Eulerian ldx dispersion / deposition model developed by the IRSN (see *Source term assessment methodology*). Subsequent RN deposition was computed assuming a dry deposition velocity of 0.2 $cm \cdot s^{-1}$. Based on actual meteorological data, the effective dose induced both by inhalation (respiratory rate of 22.18 $m^3 \cdot d^{-1}$) and ingestion of foodstuffs following RN deposition was determined to be 150 nSv for an adult (100 nSv for inhalation from April 1 to 22, 2020 and 50 nSv for ingestion over a period of 1 year after deposition). The detailed inhalation dose per radionuclide is as follows: ^{137}Cs 0.1 nSv, ^{90}Sr 1 nSv, ^{238}Pu 5 nSv, ^{239}Pu 5 nSv, ^{240}Pu 10 nSv, ^{241}Pu 5 nSv (ΣPu 25 nSv) and ^{241}Am 75 nSv. For the ingestion dose calculation, the main agricultural products that were considered include vegetables in season (April), dairy products and meat. The daily consumption of 500 g of leafy vegetables is considered as the most penalizing scenario. As confirmed by Talerko et al.,[49] the dose induced by exposure to the cloud shine (immersion) was negligible as compared with internal exposure. The total exposure was also negligible compared to the annual public exposure limit of 1 mSv according to Ukrainian Radiation Safety Standards for the general public as an added effective dose[45] or when compared to the average annual global exposure of 2.4 mSv induced by natural background radiation.[29]

Elsewhere in Europe, doses were even lower as airborne concentrations were much lower. At some distant locations the contribution of the fire plume to the ^{137}Cs airborne concentration was estimated to be between 2 and 8-fold at most the usual ^{137}Cs trace-level concentration. Assuming consistent soil contamination as a routine source of ^{137}Cs background emission (through soil particle resuspension) the use of the airborne $^{137}Cs/^{40}K$ ratio has also proven to be helpful in the determination of fire plume contribution. However, the proper use of this tool requires the knowledge of a local baseline value to distinguish any additional remote ^{137}Cs input.

In anticipation of future wildfires in the Chernobyl area, the detailed study of the re-emission into the atmosphere of Pu isotopes released during the Chernobyl accident or arising as their decay products (^{241}Am,

673 ^{237}Np), in addition to ^{90}Sr, ^{137}Cs, ^{243,244}Cm and naturally occurring radionuclides such as ^{210}Po during
674 wildfires is recommended for a more comprehensive estimate of the internal exposure by inhalation for
675 firefighters and for the population. It is also essential to point out that our knowledge of respective amounts
676 of radionuclides emitted both in gaseous phase according to their volatilization point and as aerosol particles
677 (flying ashes) is insufficient and requires further study. In the future, if forests are not thinned, exposure
678 risks from forest fire emissions are expected to increase due to the accumulation of debris, litter and standing
679 dead trees and because of early and lengthy droughts in the framework of climate change.
680 Lengthy wildfire outbreaks are a challenge for inverse modeling computation when they both vary in
681 location and magnitude. Such outbreaks are also an opportunity to strengthen international collaboration
682 between radioprotection organizations and demonstrate the benefits of rapid information sharing, which is
683 the main goal of the informal Ring of Five (Ro5) European monitoring network.
684

685 **Corresponding Author**: Olivier Masson, Email: olivier.masson@irsn.fr, ORCID:
686 https://orcid.org/0000-0001-6209-6114
687
688

689 **Author Contributions:** The manuscript was written through contributions of all authors. All authors have
690 given approval to the final version of the manuscript.
691
692

693 **Acknowledgments**

694 Authors are grateful to the following Ukrainian organizations for sharing their data and regular information
695 on the fire situation: the State Scientific and Technical Center for Nuclear and Radiation Safety (SSTC), the
696 Ukrainian Hydrometeorological Institute (UHMI), the State Specialized Enterprise Ecocentre (SSE), the
697 Central Geophysical Laboratory (CGO) in Kiev, the Rivne NPP. Authors address special thanks to
698 Intelligence System GEO (ISGEO, http://www.isgeo.com.ua/ for the provision of the ^{137}Cs contamination
699 maps. We wish also to acknowledge the NASA for fire detections through the Fire Information for Resource
700 Management System Fire Information for Resource Management System (FIRMS) and the European Space
701 Agency (ESA) for the provision of Copernicus Sentinel-2 satellite images. We also thank all the Ro5
702 members involved during this event for the effort spent to insure airborne radioactivity monitoring through
703 aerosol sampling despite social confinement during the COVID-19 pandemic, and for stimulating
704 discussions. Special thanks to Paul Kloppenberg for English corrections. This paper is dedicated to the fire
705 brigades involved during this event.
706

707 **Supporting information**

The Supporting information contains the complete airborne radionuclide concentration dataset, satellite images of fires spots and a video of the smoke plume dispersion over Europe. It also contains 1) a review of historic wildfires in contaminated ecosystems, 2) knowledge about radionuclide emission by fires in forested and non-forested lands, 3) information about long-lasting persistence of airborne ^{137}Cs at trace-levels in Europe, 4) geographic analysis and timeline of the April 2020 wilfire event in Ukraine, 5) information about the poor air quality observed in Kiev on April 16, 2020, 6) radionuclide apportionment in the terrestrial ecosystem, 7) information about data collection 8) information about the use of airborne ^{40}K and $^{137}Cs/^{40}K$ ratio for the identification of a fire plume contribution, and 9) information about the methodology used for the source term assessment.

Competing interests

The authors declare that they have no conflicts of interest.

References

1. Wotawa, G.; De Geer, L. E.; Becker, A.; D'Amours, R.; Jean, M.; Servranckx, R.; Ungar, K., Inter- and intra-continental transport of radioactive cesium released by boreal forest fires. *Geophys. Res. Lett.* **2006,** *33*, (12).
2. Budyka, A. K.; Ogorodnikov, B. I., Radioactive aerosols formed owing to fires in regions contaminated by products of Chernobyl accident. *Radiatsionnaya Biologiya. Radioekologiya* **1995,** *35*, (1), 102-112.
3. Paliouris, G.; Taylor, H. W.; Wein, R. W.; Svoboda, J.; Mierzynski, B., Fire as an agent in redistributing fallout ^{137}Cs in the Canadian boreal forest. *Sci. Total Environ.* **1995,** *160-161*, 153-166.
4. Nho, E. Y.; Ardouin, B.; Le Cloarec, M. F.; Ramonet, M., Origins of ^{210}Po in the atmosphere at Lamto, Ivory Coast: Biomass burning and Saharan dusts. *Atmos. Environ.* **1996,** *30*, (22), 3705-3714.
5. Carvalho, F. P.; Oliveira, J. M.; Malta, M., Exposure to radionuclides in smoke from vegetation fires. *Sci. Total Environ.* **2014,** *472*, 421-424.
6. Kashparov, V. A.; Zhurba, M. A.; Zibtsev, S. V.; Mironyuk, V. V.; Kireev, S. I., Evaluation of the expected doses of fire brigades at the Chornobyl exclusion zone in April 2015 [in Russian]. *Nuclear Physics and Atomic Energy* **2015,** *16*, (4), 399-407.
7. Amiro, B. D.; Sheppard, S. C.; Johnston, F. L.; Evenden, W. G.; Harris, D. R., Burning radionuclide question: What happens to iodine, cesium and chlorine in biomass fires? *Sci. Total Environ.* **1996,** *187*, (2), 93-103.
8. Dusha-Gudym, S. I., Forest fires on areas contaminated by radionuclides from the Chernobyl power plant accident. *Int. Forest Fire News* **1992,** *7*, 4.

9. Dusha-Gudym, S. I., *The Effects of Forest Fires on the Concentration and Transport of Radionuclides. Fire in Ecosystems of Boreal Eurasia*. Kluwer Academic Publishers: Dordrecht, 1996; Vol. 48.
10. Dusha-Gudym, S. I., Transport of radioactive materials by wildland fires in the Chernobyl Accident zone: How to address the problem. *Int. Forest Fire News* **2005**, 119-125.
11. Kaletnik, N. N., *Fire prevention and detection in closed zone. In: "Fire prevention, liquidation and impacts on the lands polluted by radionuclides"*. Forestry Institute of the National Academy of Sciences: Gomel, 2002; Vol. 54.
12. Paatero, J.; Vesterbacka, K.; Makkonen, U.; Kyllönen, K.; Hellen, H.; Hatakka, J.; Anttila, P., Resuspension of radionuclides into the atmosphere due to forest fires. *J. Radioanal. Nucl. Chem.* **2009,** *282*, (2), 473-476.
13. Lujaniene, G.; Šapolaite, J.; Remeikis, V.; Lujanas, V.; Jermolajev, A.; Aninkevičius, V., Cesium, americium and plutonium isotopes in ground level air of Vilnius. *Czech. J. Phys.* **2006,** *56*, (4), D55-D61.
14. Usenia, V. V.; Yurievich, N. N., The experience of Belarus in forest fire suppression [in Russian]. *Sustainable Forest Management* **2017,** *2*, 14-21.
15. Kovalets, I.; De With, G., Wildfires in the Chernobyl exclusion zone – a summary of the 2020 event. *Dutch Magazine for Radiation Protection* **2020,** *11*, 31-36.
16. Allard, G., Fire prevention in radiation-contaminated forests. *Unasylva* **2001,** *52*, (207), 41-42.
17. Ager, A. A.; Lasko, R.; Myroniuk, V.; Zibtsev, S.; Day, M. A.; Usenia, U.; Bogomolov, V.; Kovalets, I.; Evers, C. R., The wildfire problem in areas contaminated by the Chernobyl disaster. *Sci. Total Environ.* **2019,** *696*, 133954.
18. Smith, J. T.; Beresford, N. A., *Chernobyl - Catastrophe and Consequences*. Springer-Praxis Publishing: Chichester, 2005; p 327.
19. Strode, S. A.; Ott, L. E.; Pawson, S.; Bowyer, T. W., Emission and transport of cesium-137 from boreal biomass burning in the summer of 2010. *J. Geophys. Res.: Atmos.* **2012,** *117*, (D9).
20. Sorokina, L. Y.; Petrov, M. F., Changes in the structure of the land cover and fire safety of the Chernobyl exclusion zone landscapes: Assessment methods using satellites. *Ukrainian Geographical Journal* **2020**, 45-56.
21. Protsak, V. P.; Wojciechowicz, O. V.; Laptev, G. V. Estimation of radioactive source term dynamics for atmospheric transport during wildfires in Chernobyl Zone in Spring 2020. https://uhmi.org.ua/msg/fire2020/analytical.pdf (accessed March 2021).
22. Masson, O.; Piga, D.; Le Roux, G.; Mary, J.; de Vismes, A.; Gurriaran, R.; Renaud, P.; Saey, L.; Paulat, P., Recent trends and explanation for airborne ^{137}Cs activity level increases in France. *Radioprotection* **2009,** *44*, (2), 327-332.
23. SCK-CEN 1 https://www.sckcen.be/sites/default/files/files/2020-04/Forest%20fires%20Chernobyl_Radiological%20follow%20up_20200415.pdf (Accessed December 2020).
24. SCK-CEN 2 ttps://www.sckcen.be/sites/default/files/files/2020-04/Forest%20fires%20Chernobyl_Radiological%20follow%20up_20200430_1.pdf (Accessed December 2020).

25. IRSN 1 https://www.irsn.fr/EN/newsroom/News/Pages/20200415_Fires-in-Ukraine-in-the-Exclusion-Zone-around-chernobyl.aspx (Accessed December 2020).
26. IRSN 2 https://www.irsn.fr/EN/newsroom/News/Pages/20200420_Fires-in-Ukraine-in-the-Exclusion-Zone-around-chernobyl.aspx (Accessed 2020).
27. IRSN 3 https://www.irsn.fr/EN/newsroom/News/Pages/20200424_Fires-in-Ukraine-in-the-Exclusion-Zone-around-chernobyl-cesium-137-results-in-france.aspx (Accessed December 2020).
28. IRSN 4 https://www.irsn.fr/EN/newsroom/News/Pages/20200505_Fires-in-Ukraine-in-the-Exclusion-Zone-around-chernobyl-latest-news-and-consequences.aspx (Accessed December 2020).
29. UNSCEAR, *Exposures and effects of the Chernobyl accident (Annex J)*. United Nations: New York, 2000.
30. Tabachnyi, L.; Kokot, I., *Results of consequences of the fires on the radioactive contamination territories of Kyiv and Zhytomyr regions according to Hydrometeorological radiometrical network data*. IAEA: Vienna, 2020.
31. Pazukhin, E. M.; Borovoi, A. A.; Ogorodnikov, B. I., Forest Fire as a Factor of Environmental Redistribution of Radionuclides Originating from Chernobyl Accident. *Radiochemistry* **2004,** *46*, (1), 102-106.
32. Yoschenko, V. I.; Kashparov, V. A.; Protsak, V. P.; Lundin, S. M.; Levchuk, S. E.; Kadygrib, A. M.; Zvarich, S. I.; Khomutinin, Y. V.; Maloshtan, I. M.; Lanshin, V. P.; Kovtun, M. V.; Tschiersch, J., Resuspension and redistribution of radionuclides during grassland and forest fires in the Chernobyl exclusion zone: part I. Fire experiments. *J. Environ. Radioact.* **2006,** *86*, (2), 143-163.
33. Steinhauser, G., Anthropogenic radioactive particles in the environment. *J. Radioanal. Nucl. Chem.* **2018,** *318*, (3), 1629-1639.
34. IAEA, *Environmental consequences of the Chernobyl accident and their remediation: twenty years of experience. Radiological assessment reports series*. IAEA: Vienna, 2006.
35. Blake, N. J.; Blake, D. R.; Wingenter, O. W.; Sive, B. C.; McKenzie, L. M.; Lopez, J. P.; Simpson, I. J.; Fuelberg, H. E.; Sachse, G. W.; Anderson, B. E.; Gregory, G. L.; Carroll, M. A.; Albercook, G. M.; Rowland, F. S., Influence of southern hemispheric biomass burning on midtropospheric distributions of nonmethane hydrocarbons and selected halocarbons over the remote South Pacific. *J. Geophys. Res.: Atmos.* **1999,** *104*, (D13), 16213-16232.
36. Jargin, S. V., Forest fires in the former Soviet Union: no reasons for radiophobia. *J. Environ. Radioact.* **2011,** *102*, (2), 218-219.
37. Kashparov, V. A.; Lundin, S. M.; Khomutinin, Y. V.; Kaminsky, S. P.; Levchuk, S. E.; Protsak, V. P.; Kadygrib, A. M.; Zvarich, S. I.; Yoschenko, V. I.; Tschiersch, J., Soil contamination with Sr-90 in the near zone of the Chernobyl accident. *J. Environ. Radioact.* **2001,** *56*, (3), 285-298.
38. Evangeliou, N.; Eckhardt, S., Uncovering transport, deposition and impact of radionuclides released after the early spring 2020 wildfires in the Chernobyl Exclusion Zone. *Sci. Rep.* **2020,** *10*, (1), 10655.
39. State Nuclear Regulatory Inspectorate of Ukraine http://www.snrc.gov.ua/nuclear/en/publish/article/368134 (Accessed December 2020).

40. Kirieiev, S. Estimation and forecast of the impact on the radiation situation of extreme natural factors flood, wildfire, etc. http://dazv.gov.ua/images/pdf/ukraino-japonskyj-komitet/fifth/Sergii%20KIREEV.pdf (Accessed December 2020).
41. Holiaka, D.; Yoschenko, V.; Levchuk, S.; Kashparov, V., Distributions of ^{137}Cs and ^{90}Sr activity concentrations in trunk of Scots pine (Pinus sylvestris L.) in the Chernobyl zone. *J. Environ. Radioact.* **2020,** *222*, 106319.
42. AEN-OCDE, *Tchernobyl. Evaluation de l'impact radiologique et sanitaire. Mise à jour de 2002 de «Tchernobyl Dix ans déjà ».* Agence pour l'énergie nucléaire, Organisation de coopération et de développement économiques. Les éditions de l'OCDE: Paris, 2002; p 35-37.
43. Holm, E.; Rioseco, J.; Pettersson, H., Fallout of transuranium elements following the Chernobyl accident. *J. Radioanal. Nucl. Chem.* **1992,** *156*, (1), 183-200.
44. Kashparov, V. A.; Lundin, S. M.; Zvarych, S. I.; Yoshchenko, V. I.; Levchuk, S. E.; Khomutinin, Y. V.; Maloshtan, I. M.; Protsak, V. P., Territory contamination with the radionuclides representing the fuel component of Chernobyl fallout. *Sci. Total Environ.* **2003,** *317*, (1-3), 105-119.
45. Ministry of Health of Ukraine, *Radiation Safety Standards of Ukraine. NRBU-97/D-2000.* Ministry of Health of Ukraine: Kyiv, 2000.
46. Ovadnevaitė, J.; Kvietkus, K.; Maršalka, A., 2002 summer fires in Lithuania: Impact on the Vilnius city air quality and the inhabitants health. *Sci. Total Environ.* **2006,** *356*, (1), 11-21.
47. Stoulos, S.; Besis, A.; Ioannidou, A., Determination of low ^{137}Cs concentration in the atmosphere due to Chernobyl contaminated forest-wood burning. *J. Environ. Radioact.* **2020,** *222*, 106383.
48. Muramatsu, Y.; Rühm, W.; Yoshida, S.; Tagami, K.; Uchida, S.; Wirth, E., Concentrations of ^{239}Pu and ^{240}Pu and Their Isotopic Ratios Determined by ICP-MS in Soils Collected from the Chernobyl 30-km Zone. *Environ. Sci. Technol.* **2000,** *34*, (14), 2913-2917.
49. Talerko, M.; Kovalets, I.; Lev, T.; Igarashi, Y.; Romanenko, O., Simulation study of radionuclide atmospheric transport after wildland fires in the Chernobyl Exclusion Zone in April 2020. *Atmospheric Pollution Research* **2021,** *12*, (3), 193-204.
50. De Meutter, P.; Gueibe, C.; Tomas, J.; Outer, P. d.; Apituley, A.; Bruggeman, M.; Camps, J.; Delcloo, A.; Knetsch, G.-J.; Roobol, L.; Verheyen, L., The assessment of the April 2020 Chernobyl wildfires and their impact on Cs-137 levels in Belgium and The Netherlands. *J. Environ. Radioact.* **2021,** *237*, 106688.
51. Jakopič, R.; Richter, S.; Kühn, H.; Aregbe, Y., Determination of ^{240}Pu/^{239}Pu, ^{241}Pu/^{239}Pu and ^{242}Pu/^{239}Pu isotope ratios in environmental reference materials and samples from Chernobyl by thermal ionization mass spectrometry (TIMS) and filament carburization. *J. Anal. At. Spectrom.* **2010,** *25*, (6), 815-821.
52. Carbol, P.; Solatie, D.; Erdmann, N.; Nylén, T.; Betti, M., Deposition and distribution of Chernobyl fallout fission products and actinides in a Russian soil profile. *J. Environ. Radioact.* **2003,** *68*, (1), 27-46.
53. Paatero, J.; Jaakkol, T.; Reponen, A., Determination of the ^{241}Pu deposition in Finland after the Chernobyl Accident. *Radiochim. Acta* **1994,** *64*, (2), 139-144.
54. Mietelski, J. W.; Szwałko, P.; Tomankiewicz, E.; Gaca, P.; Małek, S.; Barszcz, J.; Grabowska, S., ^{137}Cs, ^{40}K, ^{90}Sr, $^{238, 239+240}$Pu, ^{241}Am and $^{243+244}$Cm in forest litter and their transfer to some

874 species of insects and plants in boreal forests: Three case studies. *J. Radioanal. Nucl. Chem.*
875 **2004,** *262*, (3), 645-660.
876 55. Ketterer, M. E.; Hafer, K. M.; Mietelski, J. W., Resolving Chernobyl vs. global fallout
877 contributions in soils from Poland using Plutonium atom ratios measured by inductively
878 coupled plasma mass spectrometry. *J. Environ. Radioact.* **2004,** *73*, (2), 183-201.
879 56. Salminen-Paatero, S.; Paatero, J.; Jaakkola, T., ^{241}Pu and ^{241}Pu/$^{239+240}$Pu activity ratio in
880 environmental samples from Finland as evaluated by the ingrowth of ^{241}Am. *Boreal Environ.*
881 *Res.* **2014,** *19*, 51-65.
882 57. Vukanac, I.; Paligorić, D.; Novković, D.; Djurašević, M.; Obradović, Z.; Milošević, Z.; Manić,
883 S., Retrospective estimation of the concentration of ^{241}Pu in air sampled at a Belgrade site
884 following the Chernobyl accident. *Appl. Radiat. Isot.* **2006,** *64*, (6), 689-692.
885 58. Sokolik, G. A.; Ovsiannikova, S. V.; Ivanova, T. G.; Leinova, S. L., Soil–plant transfer of
886 plutonium and americium in contaminated regions of Belarus after the Chernobyl catastrophe.
887 *Environ. Int.* **2004,** *30*, (7), 939-947.
888 59. Lehto, J.; Vaaramaa, K.; Leskinen, A., ^{137}Cs, ^{239,240}Pu and ^{241}Am in boreal forest soil and their
889 transfer into wild mushrooms and berries. *J. Environ. Radioact.* **2013,** *116*, 124-132.
890 60. Zheng, J.; Tagami, K.; Watanabe, Y.; Uchida, S.; Aono, T.; Ishii, N.; Yoshida, S.; Kubota, Y.;
891 Fuma, S.; Ihara, S., Isotopic evidence of plutonium release into the environment from the
892 Fukushima DNPP accident. *Sci. Rep.* **2012,** *2*, 304.
893 61. Nisbet, A. F.; Shaw, S., Summary of a 5-year lysimeter study on the time-dependent transfer
894 of ^{137}Cs, ^{90}Sr, ^{239,240}Pu and ^{241}Am to crops from three contrasting soil types: 1. Transfer to the
895 edible portion. *J. Environ. Radioact.* **1994,** *23*, (1), 1-17.
896 62. Dvornik, A. A.; Dvornik, A. M.; Korol, R. A.; Shamal, N. V.; Gaponenko, S. O.; Bardyukova,
897 A. V., Potential threat to human health during forest fires in the Belarusian exclusion zone.
898 *Aerosol Sci. Technol.* **2018,** *52*, (8), 923-932.
899 63. Buzdalkin, K. N.; Bortnovsky, V. N., *Inhalation of transuranic elements in case of*
900 *emergencies in the exclusion zone of the Chernobyl NPP. Medico-Biological and Socio-*
901 *Psychological Issues of Safety in Emergency Situations (in Russian)*. Nikiforov Russian Center
902 of Emergency and Radiation Medicine, EMERCOM of Russia: 2019.
903 64. Security, R. N. http://russiannuclearsecurity.com/wildfires-in-ukraine-draw-dangerously-
904 close-to-chernobyl-exclusion-zone (Accessed December 2020).
905 65. Antropov, V. M.; Bugai, D. A.; Dutton, L. M.; Gerchikov, M. Y.; Kennett, E. J.; Ledenev, A.
906 I.; Novikov, A. A.; Rudko, V.; Ziegenhagen, J., *Review and analysis of solid long-lived and*
907 *high level radioactive waste arising at the Chernobyl nuclear power plant and the restricted*
908 *zone*. European Commission: 2001.
909 66. Shcheglov, A.; Tsvetnova, O. g.; Klyashtorin, A., Biogeochemical cycles of Chernobyl-born
910 radionuclides in the contaminated forest ecosystems. Long-term dynamics of the migration
911 processes. *J. Geochem. Explor.* **2014,** *144*, 260-266.
912 67. Thiry, Y.; Colle, C.; Yoschenko, V.; Levchuk, S.; Van Hees, M.; Hurtevent, P.; Kashparov,
913 V., Impact of Scots pine (Pinus sylvestris L.) plantings on long term ^{137}Cs and ^{90}Sr recycling
914 from a waste burial site in the Chernobyl Red Forest. *J. Environ. Radioact.* **2009,** *100*, (12),
915 1062-1068.
916 68. Kashparov, V.; Salbu, B.; Simonucci, C.; Levchuk, S.; Reinoso-Maset, E.; Lind, O. C.;
917 Maloshtan, I.; Protsak, V.; Courbet, C.; Nguyen, H., Validation of a fuel particle dissolution

model with samples from the Red Forest within the Chernobyl exclusion zone. *J. Environ. Radioact.* **2020,** *223-224*, 106387.

69. Kashparov, V.; Salbu, B.; Levchuk, S.; Protsak, V.; Maloshtan, I.; Simonucci, C.; Courbet, C.; Nguyen, H. L.; Sanzharova, N.; Zabrotsky, V., Environmental behaviour of radioactive particles from Chernobyl. *J. Environ. Radioact.* **2019,** *208-209*, 106025.
70. ICRP 66, Human Respiratory Tract Model for Radiological Protection. *ICRP Publication* **1994,** *66*.
71. ICRP 119, Compendium of Dose Coefficients based on ICRP Publication 60. *Ann. ICRP* **2012,** *41*, 1-130.
72. ICRP 71, Age-dependent Doses to Members of the Public from Intake of Radionuclides. Part 4. Inhalation Dose Coefficients. *ICRP Publication* **1995,** *71*.
73. 134, I., Occupational Intakes of Radionuclides: Part 2. *Ann. ICRP* **2016,** *45*, 1-352.
74. Terray, L.; D'Amico, D.; Masson, O.; Sabroux, J.-C., What can gross alpha/beta activities tell about ^{210}Po and ^{210}Pb in the atmosphere? *J. Environ. Radioact.* **2020,** *225*, 106437.

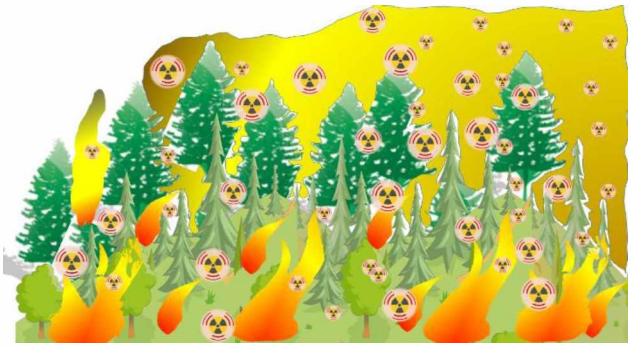

For Table of Contents only